

Review

Hepatitis C Virus Infection and Intrinsic Disorder in the Signaling Pathways Induced by Toll-Like Receptors

Elrashdy M. Redwan ^{1,2} , Abdullah A. Aljadawi ¹ and Vladimir N. Uversky ^{1,3,*} 

¹ Biological Science Department, Faculty of Science, King Abdulaziz University, P.O. Box 80203, Jeddah 21589, Saudi Arabia; iradwan@kau.edu.sa (E.M.R.); aaljaddawi@kau.edu.sa (A.A.A.)

² Therapeutic and Protective Proteins Laboratory, Protein Research Department, Genetic Engineering and Biotechnology Research Institute, City for Scientific Research and Technology Applications, New Borg EL-Arab, Alexandria 21934, Egypt

³ Department of Molecular Medicine and USF Health Byrd Alzheimer's Research Institute, Morsani College of Medicine, University of South Florida, Tampa, FL 33612, USA

* Correspondence: vuffersky@usf.edu

Simple Summary: Human hepatitis C virus causes contagious liver disease hepatitis C, which is broadly spread around the globe. Infection with this virus causes an inflammation of the liver that leads to both acute and chronic hepatitis, which, if left untreated, often results in the development of serious lifelong illnesses such as liver fibrosis, liver cirrhosis, hepatocellular carcinoma, and end-stage liver disease in humans. Toll-like receptors are a class of pattern recognition receptors that exist in liver parenchymal cells and various immune cells, and play an important role in the liver immune system by initiating multiple cellular downstream pathways in response to the recognition of pathogens such as hepatitis C virus. Proteins from the hepatitis C virus, Toll-like receptors themselves, and proteins from the pathways they activate are multifunctional. Since protein multifunctionality is commonly associated with intrinsic disorder (i.e., lack of stable 3D structures), we used an intrinsic disorder angle to examine the interplay between the hepatitis C virus infection and signaling pathways induced by Toll-like receptors. We show that almost all of these proteins contained noticeable levels of disorder, indicating that intrinsic disorder is prominently utilized in virus–host warfare.

Abstract: In this study, we examined the interplay between protein intrinsic disorder, hepatitis C virus (HCV) infection, and signaling pathways induced by Toll-like receptors (TLRs). To this end, 10 HCV proteins, 10 human TLRs, and 41 proteins from the TLR-induced downstream pathways were considered from the prevalence of intrinsic disorder. Mapping of the intrinsic disorder to the HCV-TLR interactome and to the TLR-based pathways of human innate immune response to the HCV infection demonstrates that substantial levels of intrinsic disorder are characteristic for proteins involved in the regulation and execution of these innate immunity pathways and in HCV-TLR interaction. Disordered regions, being commonly enriched in sites of various posttranslational modifications, may play important functional roles by promoting protein–protein interactions and support the binding of the analyzed proteins to other partners such as nucleic acids. It seems that this system represents an important illustration of the role of intrinsic disorder in virus–host warfare.

Keywords: intrinsically disordered region; intrinsically disordered protein; hepatitis C virus; toll-like receptors; protein–protein interactions; disorder-to-order transition; posttranslational modifications



Citation: Redwan, E.M.; Aljadawi, A.A.; Uversky, V.N. Hepatitis C Virus Infection and Intrinsic Disorder in the Signaling Pathways Induced by Toll-Like Receptors. *Biology* **2022**, *11*, 1091. <https://doi.org/10.3390/biology11071091>

Academic Editors: Luca Mollica and Gabriele Giachin

Received: 24 May 2022

Accepted: 19 July 2022

Published: 21 July 2022

Publisher's Note: MDPI stays neutral with regard to jurisdictional claims in published maps and institutional affiliations.



Copyright: © 2022 by the authors. Licensee MDPI, Basel, Switzerland. This article is an open access article distributed under the terms and conditions of the Creative Commons Attribution (CC BY) license (<https://creativecommons.org/licenses/by/4.0/>).

1. Introduction

1.1. Brief Introduction of Human Hepatitis C Virus (HCV)

Human hepatitis C virus (HCV), which causes the contagious liver disease hepatitis C, is one of the best known members of the *Hepacivirus* genus of the *Flaviviridae* family of small enveloped RNA viruses. The capsids of these spherical viruses range in diameter between 40 and 60 nm, and their genomes represent single-stranded positive-sense RNA

containing 9.6 to 12.3 kb. In addition to HCV, the *Hepacivirus* genus includes hepatitis G virus (HGV, also known as the GB virus B (GBV-B)), bat hepacivirus, canine hepacivirus, horse hepacivirus, and rodent hepacivirus. Furthermore, there are three other genera in the *Flaviviridae* family, with many viruses from this family predominantly spread by mosquitoes and ticks. In the *Flavivirus* genus, there are almost 70 human and animal viruses, the best-known being Alkhurma hemorrhagic fever virus (AHFV), Dengue virus (DENV), Japanese encephalitis virus (JEV), Kyasanur Forest disease virus (KFDV), Omsk hemorrhagic fever virus (OHFV), West Nile virus (WNV), yellow fever virus (YFV), and Zika virus (ZKV). The *Pegivirus* genus includes GBV-A, GBV-C, and GBV-D (the GB in their names and in GBV-B is related to the initials of the surgeon with acute hepatitis, whose serum, being inoculated into tamarins, induced hepatitis [1,2]). Finally, in the *Pestivirus* genus, one might find atypical porcine pestivirus, Aydin-like pestivirus, bovine viral diarrhea viruses 1 and 2 (BVDV-1 and BVDV-2), border disease virus (BDV), Bungowannah virus, classic swine fever virus (CSFV), Dongyang pangolin virus (DYPV), giraffe pestivirus, Hobi-like pestivirus, pronghorn pestivirus, and rat pestivirus.

Since the liver parenchymal cells represent the preferential sites of the HCV replication, infection with this virus causes an inflammation of the liver that leads to both acute and chronic hepatitis, which, if left untreated, often results in the development of serious lifelong illnesses such as liver fibrosis, liver cirrhosis, hepatocellular carcinoma, and end-stage liver disease in humans [3]. Although in developed and developing countries, HCV is predominantly transmitted via needle sharing during intravenous drug use and unsafe medical procedures (blood transfusion, organ transplantation, contaminated medical instruments, accidental needle stick injury in health care workers), respectively [4], there are other routes of virus transmission via inadvertent exposure to infected blood such as body modification (tattooing and piercing), sexual intercourse, sharing of personal items, and passage from an infected mother to unborn child (vertical transmission).

According to the World Health Organization (WHO) [5], HCV chronically infects 58 million people worldwide, with about 1.5 million new infections occurring per year. Furthermore, HCV continues to be a leading cause of liver-related mortality worldwide, causing 333,000, 499,000, and 704,000 deaths in 1990, 2010, and 2013, respectively [6–8]. Chronic HCV infection rates are unevenly distributed around the globe. In fact, although the total global HCV prevalence is estimated to be 2.5% (177.5 million of HCV infected adults) [9], and although the prevalence of chronic hepatitis C is generally below 2% in high income countries [10,11] (though even in these countries, prevalence of viremic HCV infection ranges from 0.4% (Austria, Cyprus, Germany, Denmark, France, the UK) to 1.5% (Israel, Italy) [11]); in many low-middle income countries, HCV prevalence exceeds 5% [6]. For example, up to 22% of Egypt's population is chronically infected with this virus [11,12]. Some other countries with high HCV prevalence ($\geq 5\%$) are Cameroon at 4.9–13.8% [13], Gabon at 4.9–11.2% [14], Georgia at 6.7% [15], Mongolia at 9.6–10.8% [16,17], Nigeria at 3.1–8.4% [13], Pakistan at 6.8% [18], and Uzbekistan at 11.3% [10].

Several factors define the high variability of the HCV genome. An incomplete list of factors that constantly influence HCV evolution and shape the genome of this virus includes peculiarities of the environment, host genotypic variation, and the lack of a proofreading mechanism during replication [19,20]. As a result, HCV is characterized by the high genetic heterogeneity, and one can find seven major HCV genotypes (1–7) [21] with an average difference of 30% at the nucleotide level [22]. These genotypes are further subdivided into 86 subtypes [23], which are unevenly distributed between genotypes [24], and which, at the nucleotide level, show a difference ranging between 15 and 25% [22]. Similar to the uneven worldwide distribution of global HCV infection, genotypes are distributed disproportionally within the infected population, with the geographic regions being characterized by different relative prevalence of the HCV genotypes. One of the illustrations of such disproportional distribution is given by the United States, where genotypes 1 and 2 are found in 70% and 20% of HCV cases, respectively, with other genotypes each accounting for $\sim 1\%$ [25]. However, the Swat of Khyber Pakhtoonkhaw

district of Pakistan was characterized by a very different distribution, where 3a was the most prevalent HCV genotype (34.1%), followed by 2a (8.1%), 3b (7%), and 1a (5.4%) [26].

Furthermore, although genotype 1 is the most common cause of the HCV infection in South America and Europe [3], in South Africa and Hong Kong, the commonly found genotypes are 5 and 6, respectively, whereas HCV-4 is the most common genotype in North Africa and the Middle East [22,27]. Curiously, several specific geographical locations are characterized by unique non-common HCV genotypes. These include Vietnam, where patients are commonly infected with the HCV genotypes 7, 8, and 9 [28,29], and by Indonesian patients with a wide distribution of genotypes 10 and 11 [30]. Finally, the HCV subtypes are also disproportionately distributed among different geographical locations. For example, Japanese patients are preferentially infected by the HCV subtype 1b [31], whereas the most common subgenotypes found in European and U.S. patients are the HCV subtypes 1a and 1b [32–34]. Similarly, although HCV subtype 2c is exclusively found in Northern Italy, North America, Europe, and Japan, they are also places where the most commonly found HCV subtypes are 2a and 2b [31–33,35]. Another important mechanism allowing HCV to efficiently escape the host immune response and complicating the development of vaccines against this virus is the error-prone RNA polymerase-triggered generation of quasi-species in infected individuals [36].

HCV is an RNA virus with a single-stranded positive-sense RNA genome containing a single 9600-nucleotide-long open reading frame [37] encoding a ~3010-residue-long polypeptide known as the HCV genome polyprotein [38]. Processing of this polyprotein through viral and cellular proteases generates ten HCV proteins with various vital roles in the viral replication and viral particle assembly within the host cell [38]. Some of these proteins such as core or nucleocapsid protein C (p22) and envelope glycoproteins E1 (or gp35) and E2 (or gp70) are structural proteins that assemble to form the viral capsid surrounding and protecting the viral genomic RNA. These structural proteins are released from the HCV genome polyprotein by the host endoplasmic reticulum (ER) signal peptidase(s) [39]. The remaining HCV proteins are non-structural proteins, which are required for viral replication and are released from the polyprotein by the cleavage action of the HCV proteases NS2-3 and NS3-4A [38,39]. These non-structural proteins are a viral channel forming protein p7, transmembrane protein NS2 (p23), protease/RNA helicase NS3 (p70), cofactor NS4A (p8), cofactor NS4b (p27), interferon resisting protein NS5A (p56), and RNA polymerase NS5B (p68) [38]. Importantly, similar to proteins from other viruses, all HCV proteins are multifunctional and are characterized by high binding promiscuity [40,41], which is illustrated by Figure 1, showing the interactions between the HCV and host cell proteins [41].

1.2. Introduction of the Protein Intrinsic Disorder Phenomenon

It is recognized that the robustness, multifunctionality, and binding promiscuity of viral proteins can be attributed to their unique structural features and characteristics [42] such as significant enrichment in polar residues and depletion in hydrophobic residues [43], relatively low package density, an increased fraction of residues not involved in secondary structure elements, relatively weak network of inter-residue interactions, lower destabilizing effects of mutations [42], and an abundant presence of partially folded, incompletely ordered, or intrinsically disordered domains and regions that grant structural and functional flexibility to proteins carrying them [44]. This is in line with the current understanding of the protein sequence–function relationship, where protein functionality is not necessarily dependent on a unique 3D-structure, and many biologically active proteins are completely or partially disordered [45–53].

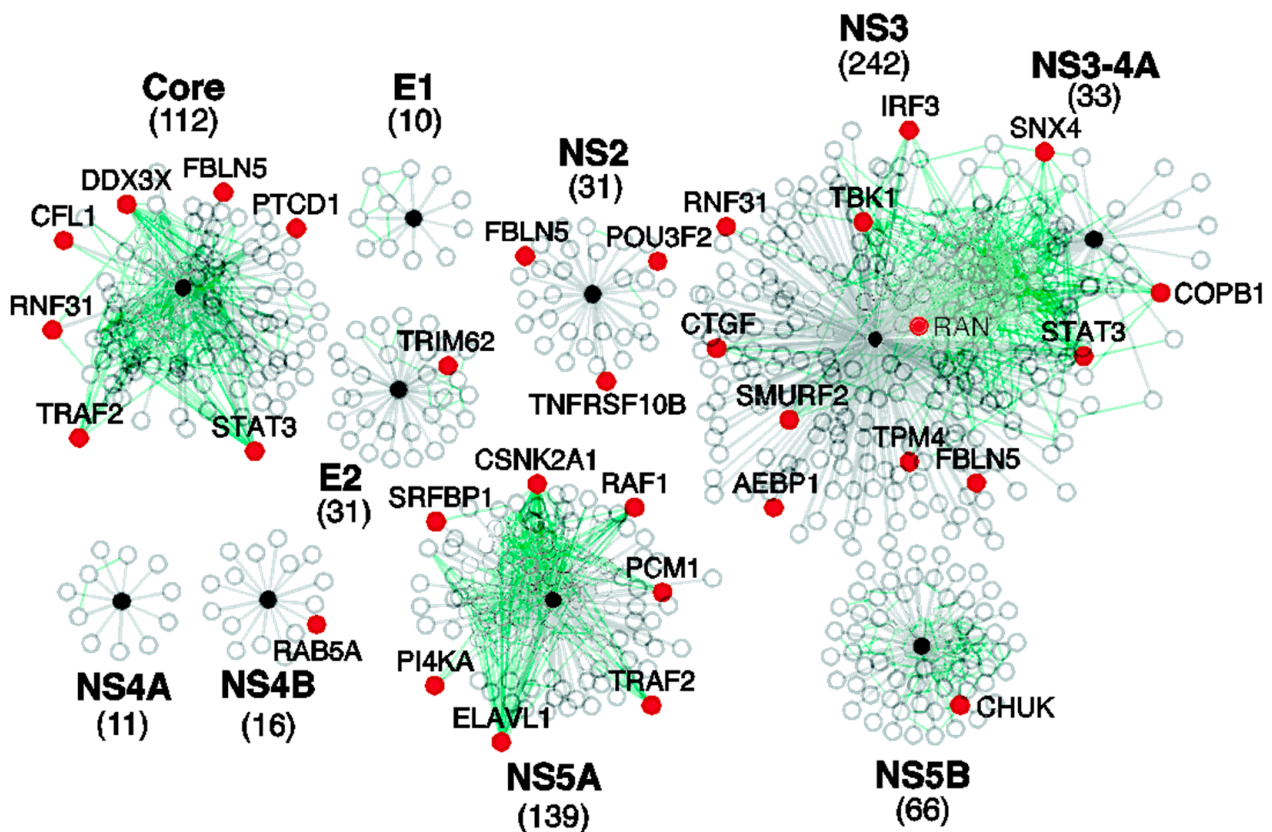


Figure 1. The interactions between HCV and cellular proteins. HCV-human protein–protein interactions (grey lines) were downloaded from the HCVPro database [54] and deduced from references [55,56]. The black spheres represent HCV proteins, the white spheres indicate cellular proteins that bind to HCV proteins, and the red spheres signify human proteins that bind to HCV proteins and were implicated in HCV replication by at least one large-scale siRNA screen. The green lines represent interactions between cellular proteins that bind to HCV proteins. The total number of cellular proteins that bind to each HCV protein is shown in parentheses beneath the protein name. Reproduced from [41] with permission from the Royal Society of Chemistry.

Such functional intrinsically disordered proteins (IDPs) and regions (IDRs) do not have stable 3D structures, being present instead as highly dynamic conformational ensembles [45,47,51,57–60]. Intrinsic disorder in proteins comes in multiple flavors, and entire protein or protein regions can be disordered to different degrees, existing as collapsed, semi-collapsed, or extended conformational ensembles with molten globule-like, pre-molten globule-like, and coil-like properties [48,50,60,61]. Overall, any protein can be considered as an ensemble of units capable of independent folding (foldons), IDRs undergoing disorder-to-order transitions induced by binding to specific partners (inducible foldons), IDRs with the capability to fold differently being bound to different partners (morphing inducible foldons), permanently disordered regions (non-foldons), regions with perpetually semi-folded conformations (semi-foldons), and ordered regions, the functional activation of which requires order-to-disorder transitions (unfoldons) [60,62–64]. This structural heterogeneity of proteins is related to their multifunctionality via the structure–function continuum model, which is based on the “one gene–many proteins–many functions” concept, instead of the classical “lock-and-key” theory rooted in the long-accepted “one gene–one protein–one structure–one function” view [65,66]. In fact, IDPs/IDRs are commonly related to the regulation of cell signaling, are involved in a multitude of recognition events, and play important roles in controlling various pathways [47,50,52,60,67–76], and thereby complement catalytic and transport activities traditionally attributed to ordered

proteins [58,77–80]. Furthermore, these multifunctional flexible proteins are commonly related to the pathogenesis of various human diseases [81,82].

It is now recognized that IDPs/IDRs are not mere exceptions that are rarely found within the functional universe of ordered proteins, where a unique structure defines the unique function. Instead, they are very abundant in all proteomes analyzed so far [45,46,49,50,53], with the largest variability in the proteome-wide content of disordered residues being found in viral proteomes [83,84]. Recently, the abundance of intrinsic disorder in the completed proteomes of several human HCV genotypes (such as 1a, 1b, 1c, 2a, 2b, 2c, 2k, 3a, 3b, 3k, 4a, 5a, 6a, 6b, 6d, 6g, 6h, and 6k) was evaluated using a wide spectrum of bioinformatic techniques [41]. This analysis was complemented by the investigation of the peculiarities of disorder distribution within the individual HCV proteins, which helped establish a potential conjunction between the structural disorder and functions of the ten HCV proteins [41]. This analysis revealed that “intrinsic disorder or increased flexibility is not only abundant in these proteins, but is absolutely necessary for their functions, playing a crucial role in the proteolytic processing of the HCV polyprotein, the maturation of the individual HCV proteins, and being related to the posttranslational modifications of these proteins and their interactions with DNA, RNA, and various host proteins” [41]. In line with these previous studies, our analysis (see below) showed that HCV contains four ordered proteins (E1, E2, NS2, and NS4B), five moderately disordered proteins (p7, NS3, NS4A, and NS5B), and two highly disordered proteins (core and NS5A).

2. TLRs, Important Players of the Liver Immune System

Toll-like receptors (TLRs), a class of pattern recognition receptors, exist in liver parenchymal cells and various immune cells, and serve as important members of the liver immune system [20], playing a number of vital roles in both inflammatory and infectious diseases [85,86]. In fact, these receptors are known to improve the overall efficiency of the immune response, being able to mediate innate immunity and induce acquired immunity. In innate immunity, the main functions of TLRs are related to the recognition of danger-associated molecular patterns (DAMPs) and pathogen-associated molecular patterns (PAMPs) [87]. Recognition of PAMPs and DAMPs by TLRs initiates a cascade of events that eventually results in the killing of a microbe. The corresponding events range from the recruitment of phagocytes to the site of infection to the initiation of the expression of chemokines and cytokines acting as inflammatory mediators [88,89].

There are ten TLRs (TLR1 through TLR10) in humans [90–94], which are differently distributed within a cell and can be further grouped based on their cellular location, with TLR1, TLR2, TLR4, TLR5, TLR6, and TLR10 being found on the plasma membrane, and TLR3, TLR7, TLR8, and TLR9 being located on the endosomal membranes [20,93,94]. Importantly, this diversity of human TLRs is determined by the need to recognize a multitude of the PAMPs from bacteria, fungi, protozoa, and viruses [89,90,93], with each TLR being able to sense a specific set of PAMPs. Here, the nucleic components of pathogens are mainly recognized by the endosomal TLRs, where double-strand RNA, single-stranded RNA, and CpG DNA are sensed by TLR3, TLR7/TLR8, and TLR9, respectively [89,90,93–95]. In response to their corresponding PAMPs, these TLRs stimulate the production of type 1 interferons (IFN1 α and IFN1 β) [96]. As far as extracellular TLRs are concerned, they can sense a broad range of PAMPs, with TLR5 sensing flagellin and TLR4 recognizing many different PAMPs such as lipopolysaccharides and taxol [89,91]. PAMP-induced activation of these TLRs at the plasma membrane triggers the activation of nuclear factor- κ B (NF- κ B) and other transcription factors that lead to the expression of several proinflammatory cytokines [97].

TLRs are involved in the interaction with each other (in fact, activation of these receptors is associated with their homo- and heterodimerization) and a multitude of human proteins. This is illustrated by Figure 2, which shows the internal and external protein–protein interaction (PPI) networks of these proteins. This analysis revealed that TLRs form a densely connected network, where, on average, each protein interacts with at least eight

partners. The most connected are TLR1, TLR7, and TLR9, which are expected to interact with all of the remaining TLRs, and the least connected is TLR10, interacting with TLR1, TLR2, TLR3, TLR5, TLR7, and TLR9 (see Figure 2A). As a group, TLRs form an immense PPI network, where one can find 459 proteins (see Figure 2B). In line with these observations, STRING-based analysis of the interactivity revealed that individual TLRs are engaged in multiple PPIs (see Table S1 and corresponding plots in the Supplementary Figure S1).

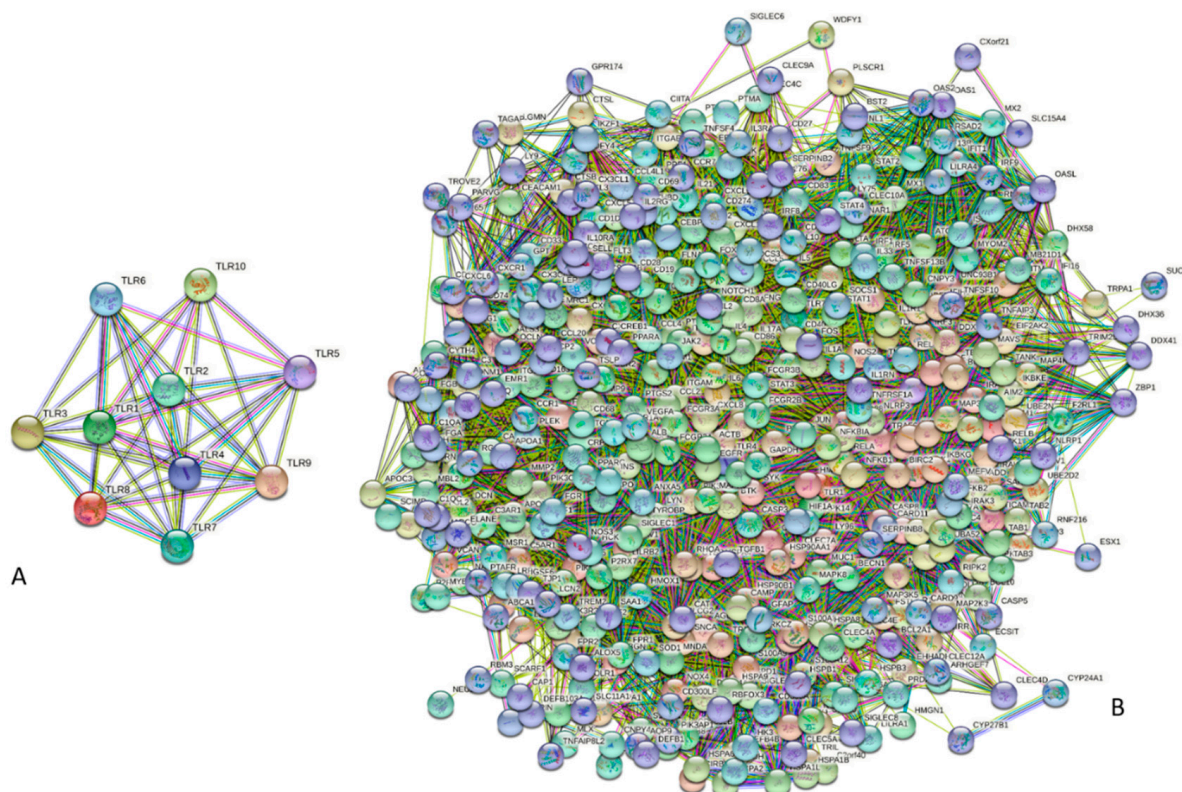


Figure 2. The internal (A) and external PPI networks (B) of human TLRs generated by STRING (Search Tool for the Retrieval of Interacting Genes, <http://string-db.org/> accessed on 7 July 2022) designed to show the predicted and experimentally-validated interactions of a protein of interest [98]. In the internal network, TLRs are connected by 41 interactions, where each TLR, on average, interacts with eight partners. In the external PPI network, 10 TLRs interact with 449 partners, which are connected by 11,715 binary PPIs. The average node degree of these network is 51 (i.e., each member of this network is expected to interact with 51 partners). Amino acid sequences of the HCV polyprotein genotype 1a (isolate H77), mature individual HCV proteins, human TLRs, and 41 major players of TLR-triggered downstream pathways were retrieved from UniProt (<https://www.uniprot.org/> accessed on 7 July 2022) [99]. Corresponding information is included in the Supplementary Figure S1. Search Tool for the Retrieval of Interacting Genes; STRING, <http://string-db.org/> accessed on 7 July 2022 [98], was used to obtain information on the interactability of HCV proteins, human TLRs, and 41 major players of TLR-triggered downstream pathways. The STRING output represents a network of predicted and experimentally-validated protein–protein interactions using seven types of evidence such as co-expression evidence (black line), co-occurrence evidence (blue line), neighborhood evidence (green line), database evidence (light blue line), experimental evidence (purple line), fusion evidence (red line), and text mining evidence (yellow line) [98]. The protein–protein interaction networks of all query proteins are shown in the Supplementary Figure S1.

A detailed description of the functional peculiarities of TLRs was outside the scope of this article, and interested readers can find related information in numerous reviews dedicated to this important family of pattern recognition receptors (e.g., see [100–117]). However, the data presented here indicate that TLRs belong to the category of multifunc-

tional proteins. It is likely that this multifunctionality is somehow encoded in the structures of these proteins.

3. Structure and Intrinsic Disorder in TLRs and Major Players in the TLR-Triggered Cellular Pathways

TLRs are type I (single-pass) transmembrane glycoproteins consisting of three functional domains such as an N-terminal extracellular (or extra-endosomal) leucine rich repeat domain (LRR domain also known as ectodomain) responsible for the recognition of PAMPs and DAMPs, a transmembrane domain (containing an α -helix, which is 21-residue-long in all human TLRs) responsible for the membrane anchoring of TLRs needed for the maintenance of their functional topologies, and a C-terminal intracellular (intraendosomal) Toll/interleukin-1 receptor (TIR) domain with a crucial role in transmitting the extracellular/extraendosomal signals into the cell or endosome [118–120]. Ligand binding to ectodomains induces their homo- or heterodimerization, which triggers dimerization of the TIR domains [118]. Activated TLR homo- and heterodimers are characterized by a strikingly similar “M”-like shape, where the C-terminal regions of the ectodomains converge in the middle [118]. This ligand-induced dimerization triggers the recruitment of various adaptor proteins to the intracellular TIR domains of TLRs, thereby initiating corresponding signaling pathways [121].

The LRR domain contains a series of 16–28 repeated LRR modules [122], with each LRR module being 20–30 residues in length and containing a conserved “LxxLxLxxN” motif and a variable part [123,124]. The conserved sequence patterns in the LRR modules define the capability of LRR proteins to fold into the unique horseshoe-like solenoid shape, where the inner concave surface is formed by the “LxxLxLxxN” motives organized in parallel β strands, and the outer convex surface originates from the variable parts of the LRR modules forming α -helices, β -turns, and/or loops [123,124]. Not all LRR modules are made equal, and some LRR proteins contain N- and C-terminally located LRRNT and LRRCT modules that often possess clusters of cysteine residues forming disulfide bridges, but not including LRR motives [123,124].

Human TLR1, TLR2, TLR3, TLR4, TLR5, TLR6, TLR8, and TLR10 contain 19, 19, 22, 18, 19, 19, 23, and 15 LRR modules, and their LRRCT modules are 55-, 55-, 54-, 51-, 53-, 55-, 53-, and 55-residues-long. The 28-residue-long LRRNT module is present only in TLR3, whereas TLR7 and TLR9, being among the longest human TLRs (see Supplementary Table S1), contain 27 and 24 LRR modules, respectively, but do not have LRRNT and LRRCT modules. Based on their structural patterns and sequences, TLRs belong to the “typical” subfamily of the LRR family proteins that contain 24-residue-long LRR modules with the conserved motif “xLxxLxxLxLxxNxLxxLPxxxFx” and that, in the convex region of their horseshoe-like structure, contain parallel 3_{10} helices [122–124]. A more detailed description of the structural peculiarities of the LRR domains can be found elsewhere [118,125].

The TIR domains are ~150-residue-long intracellular/intraendosomal TIR domains of TLRs characterized by the common fold, where one can find five α -helices surrounding a five-stranded β -sheet [118]. Based on the results of the mutational and molecular dynamic simulation analyses, it was concluded that the loop connecting the second β -strand and the second α -helix (so-called BB loop) is crucial for the TIR dimerization and/or recruitment of specific adaptor proteins [118,126] such as MyD88, MAL (also known as TIRAP), TRIF, and TRAM [121]. Importantly, since these adaptor proteins also possess TIR domains, the activation of TLR signaling is critically dependent on TIR–TIR interactions between the receptor–receptor, receptor–adaptor, and adaptor–adaptor [127].

Although ordered ectodomains and TIR domains of TLRs are well-studied, there is almost no information on the prevalence and potential functionality of intrinsically disordered and flexible regions in these proteins. To fill this gap, we conducted a multifactorial analysis of the intrinsic disorder predisposition of these important proteins. This analysis revealed that human TLRs contain multiple IDRs, some of which can be relatively long. For example, the longest IDRs in TLR3 and TLR8 have 58 and 59 residues, respectively, the

longest IDRs in TLR1 and TLR2 are 39-residues-long, whereas TLR7 has two 33-residue-long IDRs (see Table S1 and the corresponding plots in Supplementary Figure S1). Overall, Table S1 shows that, based on their intrinsic disorder content, human TLRs can be arranged as follows: TLR5 < TLR6 < TLR10 < TLR4 < TLR9 < TLR1 < TLR7 < TLR3 < TLR2 < TLR8. The first four TLRs in this list are expected to be mostly ordered, whereas the remaining six TLRs are predicted as moderately disordered (see Supplementary Table S1).

Figure 3 provides the results of the global analysis of the intrinsic disorder predisposition of human TLRs and some major members of the TLR-based signaling cascades. In addition to the utilization of protein disorder status classification based on their PPIDR values (see above), proteins can be classified using their levels of average disorder score (ADS), as highly ordered ($ADS < 0.15$), moderately disordered (ADS between 0.15 and 0.5), and highly disordered ($ADS \geq 0.5$). Figure 3A shows the correlation between the ADS and PPIDR values for the human proteins analyzed in this study.

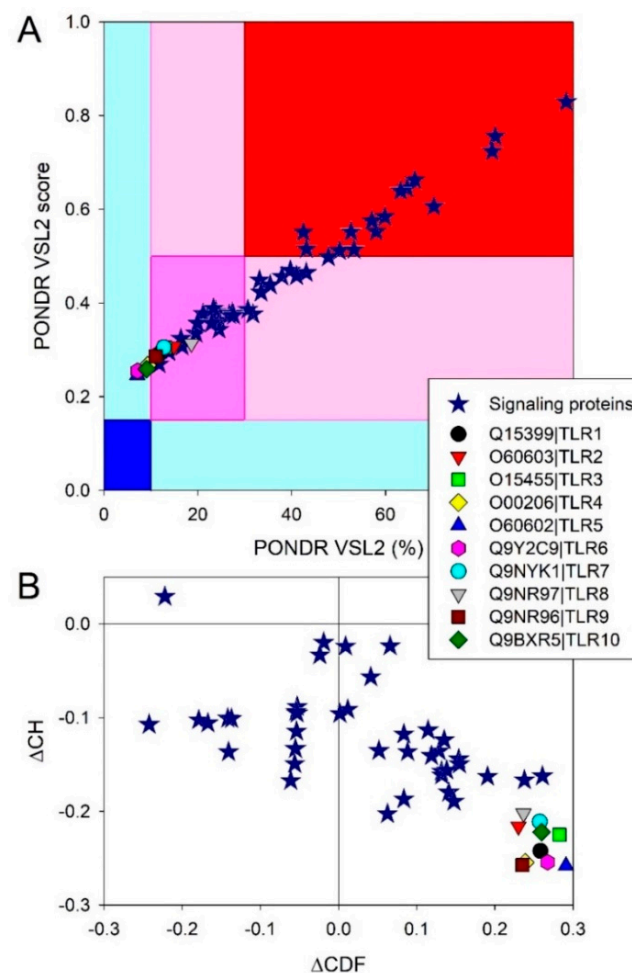


Figure 3. The global intrinsic disorder predisposition of human TLRs and major players in the TLR-triggered cellular pathways. (A) Analysis of 10 TLRs and 41 human proteins involved in TLR signaling based on the average disorder score (ADS) and percent of predicted disordered residues (PPIDR) as evaluated by PONDNR[®] VSL2 [128]. Larger values of each parameter correspond to a larger disorder propensity. Different color blocks indicate regions containing proteins with different levels of ordered, where mostly ordered, moderately disordered, and mostly disordered proteins are located within the blue, pink, and red blocks, respectively. If the two parameters (ADS and PPIDR) agree, the corresponding part of the background is shown by a dark color (blue or pink), whereas the light blue and light pink reflect areas in which only one of these criteria applies. (B) CH-CDF plot

for 10 human TLRs and 41 major players of the TLR-based signaling. Intrinsic disorder predisposition analysis of all proteins was conducted using RIDAO web crawler, which aggregates the outputs of six well-known disorder predictors: PONDR[®] VLXT [129], PONDR[®] VL3 [130], PONDR[®] VLS2 [131], PONDR[®] FIT [132], IUPred2 (Short), and IUPred2 (Long) [133,134], and also provides the mean disorder predictions for query proteins by averaging the outputs of these six predictors. The corresponding disorder profiles of all query proteins are shown in the Supplementary Figure S1. For each query protein, the predicted percentage of intrinsically disordered residues (PPIDR; i.e., percent of residues with disorder scores exceeding 0.5) was calculated based on the outputs of PONDR[®] VLS2, which is characterized by high predictive power, as evidenced by the results of the recently conducted ‘Critical assessment of protein intrinsic disorder prediction’ (CAID) experiment, where the tool was recognized as predictor #3 of the 43 evaluated methods [135]. Global disorder status of the query proteins was checked by a CH–CDF analysis [136–139] that combines the outputs of two binary predictors, the charge–hydropathy (CH) plot [51,140] and the cumulative distribution function (CDF) plot [136,140,141], to create a CH–CDF phase space, where proteins are classified as ordered (proteins predicted to be ordered by both binary predictors), putative native “molten globules” or hybrid proteins (proteins determined to be ordered/compact by CH, but disordered by CDF), putative native coils and native pre-molten globules (proteins predicted to be disordered by both methods), and proteins predicted to be disordered by CH-plot, but ordered by CDF.

This analysis revealed that no TLRs can be classified as very structured, since none of these proteins are located within the dark blue region, and only four proteins (TLR4, TLR5, TLR6, and TLR10) can be considered as mostly disordered, with the remaining TLRs being moderately disordered. Further analysis of the global intrinsic disorder predisposition of these proteins is illustrated by Figure 3B, which shows the corresponding charge-hydropathy (CH)–cumulative distribution function (CDF) plot. Here, proteins are classified based on their position within the quadrants of the CH–CDF phase space, where ordered proteins are located within the lower-right quadrant, native molten globules and/or hybrid proteins containing sizable levels of order and disorder are grouped within the lower-left quadrant, and native coils or native pre-molten globules (i.e., highly disordered proteins with extended disorder) are found within the upper-left quadrant [138]. As per the results of this analysis, all TLRs were grouped within the lower-right quadrant, confirming that these proteins were mostly ordered.

To show the peculiarities of the structure and disorder distribution within the human TLRs, we modeled their structures by AlphaFold [142] and also used the D²P² database to generate functional disorder profiles of these proteins [143]. Figure 4 gives an illustration of this analysis, showing the corresponding results for TLR5 and TLR8 as the most ordered and most disordered human TLRs. Analogous information for other TLRs is presented in the Supplementary Figure S1.

Figure 4 shows that proteins that contain both disordered regions and disorder or structural flexibility might have some functional implications (e.g., be involved in post-translational modifications). The involvement of disorder/flexibility in PTMs is supported by the fact that in TLR5, Asn residues 37, 46, 245, 342, 422, 595, and 598, which are subjected to N-linked glycosylation [144], are characterized by the local disorder scores of 0.051, 0.259, 0.279, 0.146, 0.181, 0.097, and 0.150, respectively, and the phosphorylatable residues Tyr798 [145] and Ser805 [146] showed local disorder scores of 0.411 and 0.328, respectively. In TLR8, the situation was even more dramatic, as Asn residues 29, 42, 80, 88, 115, 160, 247, 285, 293, 358, 362, 395, 416, 443, 511, 546, 582, 590, 640, 680, and 752, which were subjected to glycosylation, showed local disorder scores of 0.542, 0.620, 0.368, 0.439, 0.542, 0.234, 0.198, 0.133, 0.368, 0.344, 0.344, 0.254, 0.150, 0.706, 0.234, 0.422, 0.150, 0.247, 0.235, 0.082, and 0.672, respectively. This is in line with previous observations indicating that high levels of disorder or structural flexibility in proteins often serve as a signal for a variety of posttranslational modifications [147–149].

At the next stage, we looked at the intrinsic disorder status of major players of the TLR-initiated signaling cascades. Results of the corresponding analyses are summarized

in Table S1, Figure 3, and the corresponding plots in the Supplementary Figure S1 and show that all 41 proteins are expected to contain noticeable levels of intrinsic disorder. In fact, 13 of these proteins are predicted to have more than 50% disordered residues, and another 16 proteins possessed PPIDR values exceeding 25%, whereas disorder content in the remaining 12 proteins ranged from 10.62% (serine/threonine-protein kinase TBK1; TANK-binding kinase 1) to 24.56% (inhibitor of nuclear factor- κ B (NF- κ B) kinase subunit alpha, IKK α). Similarly, in the CH-CDF plot (see Figure 3B), one of the members of the TLR signaling cascades was predicted as highly disordered, 17 were expected to have a molten globular or hybrid structure, and 23 were mostly ordered.

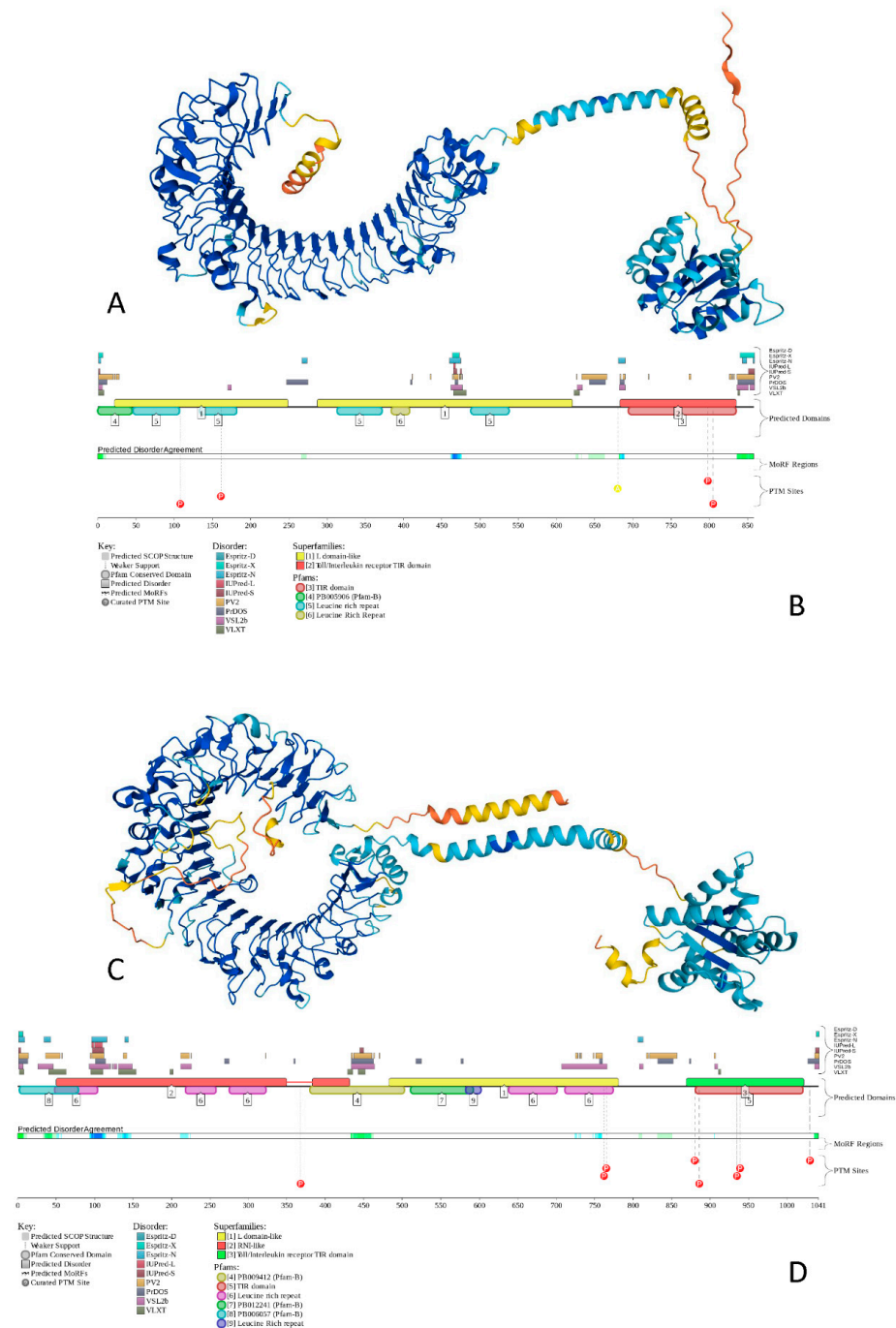


Figure 4. The structure and functional disorder of the most ordered (TLR5, plots (A,B)) and most disordered (TLR8, plots (C,D)) human TLRs. Structures of these proteins (plots (A,C)) were modeled using AlphaFold [142], which is recognized now as a highly accurate tool suitable for large-scale

structure prediction [150]. The modeled structures of all of the query proteins (HCV proteins, human TLRs and 41 major players of TLR-triggered downstream path-ways) are shown in the Supplementary Figure S1. Structural elements in these structures are colored based on the confidence of the structure prediction by AlphaFold, where dark blue and cyan segments correspond to structures predicted with high to very high confidence, whereas yellow and orange segments showed structures predicted with low to very low confidence, and which are expected to be unstructured in isolation. Functional disorder profiles (plots (B,D)) for these proteins were generated using the D²P² platform (<http://d2p2.pro/> accessed on 7 July 2022), which is a database of the predicted disorder for proteins from completely sequenced genomes [143]. Here, the outputs of IUPred [133], PONDR[®] VLXT [129], PrDOS [151], PONDR[®] VSL2B [130,152], PV2 [143], and ESpritz [153] were used to show the disorder predispositions. Consensus between these nine disorder predictors is shown by the blue-green-white bar, whereas the location of various posttranslational modifications (PTMs) is shown by differently colored circles. The platform also shows the positions of the functional SCOP domains [154,155] predicted by the SUPERFAMILY predictor [156]. Positions of these functional domains are shown below the outputs of nine disorder predictors. The functional disorder profile also includes information on the location of the predicted disorder-based binding sites (MoRF regions) identified by the ANCHOR algorithm [157] and various PTMs assigned using the outputs of the PhosphoSitePlus [158]. The functional disorder profiles of all query proteins are shown in the Supplementary Figure S1.

The most disordered TLR signaling proteins with a PPIDR exceeding 70% were the inhibitor of the nuclear factor- κ B (NF- κ B) kinase subunit gamma (IKK γ ; PPIDR = 98.57%; note that IKK γ is commonly known as NF-kappa-B essential modulator NEMO), two members of the AP-1 complex, protein c-FOS (PPIDR = 83.42%) and transcription factor Jun (PPIDR = 82.78%), and TRAF family member-associated NF-kappa-B activator (TANK, PPIDR = 70.35%).

These four proteins were selected for more in-depth disorder analysis, which is summarized in Figures 5–7. Figure 5 represents the model 3D-structures generated for these proteins by AlphaFold and clearly shows that none of them are expected to have a compact globular structure.

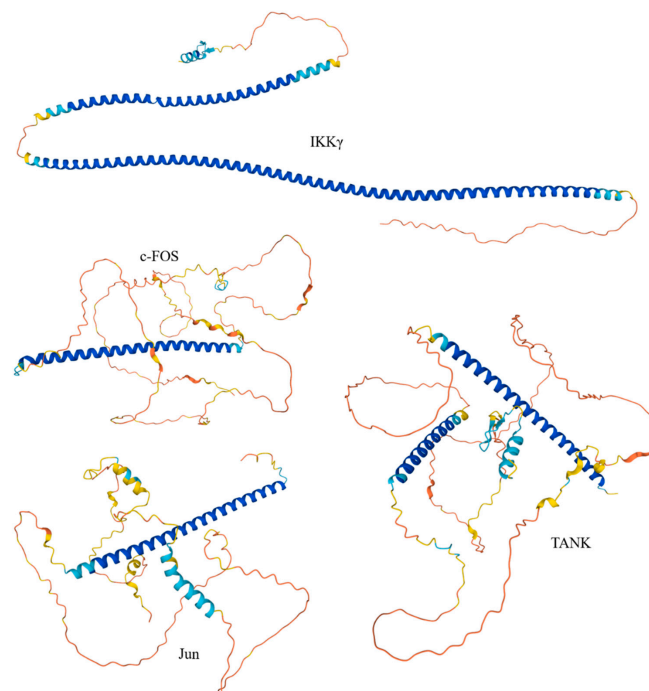


Figure 5. The 3D-structures modeled for human IKK γ , c-FOS, Jun, and TANK by AlphaFold [142]. Note the absence of the compact globular core in these proteins.

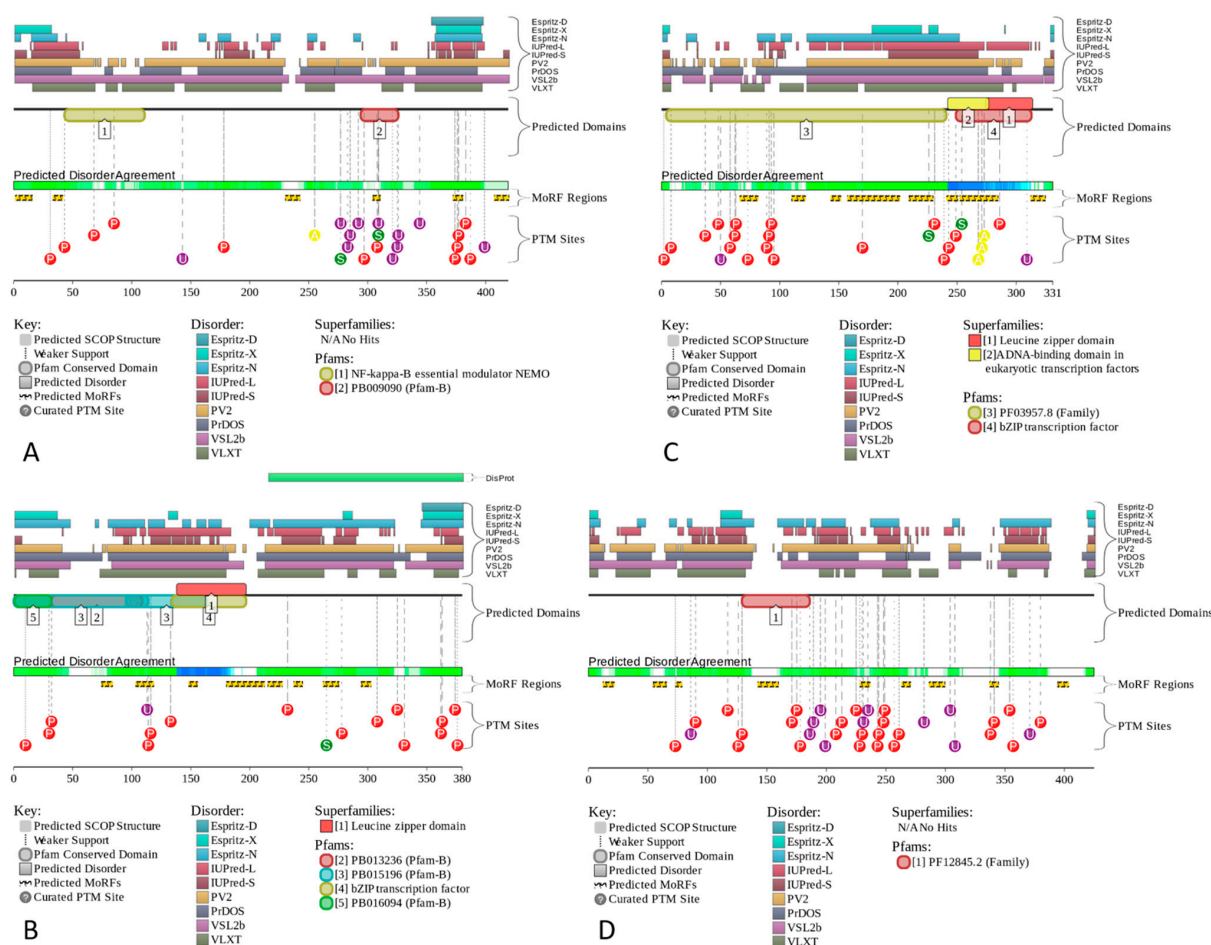


Figure 6. The functional disorder profiles generated for IKK γ (A), c-FOS (B), Jun (C), and TANK (D) using the D²P² platform (<http://d2p2.pro/> accessed on 7 July 2022). In addition to the outputs of nine disorder predictors, the positions of the conserved functional domains, consensus disorder score, and positions of the various PTMs, this plot also includes the locations of the predicted disorder-based binding sites (MoRF regions) identified by the ANCHOR algorithm [157] (shown by the yellow zigzagged bars).

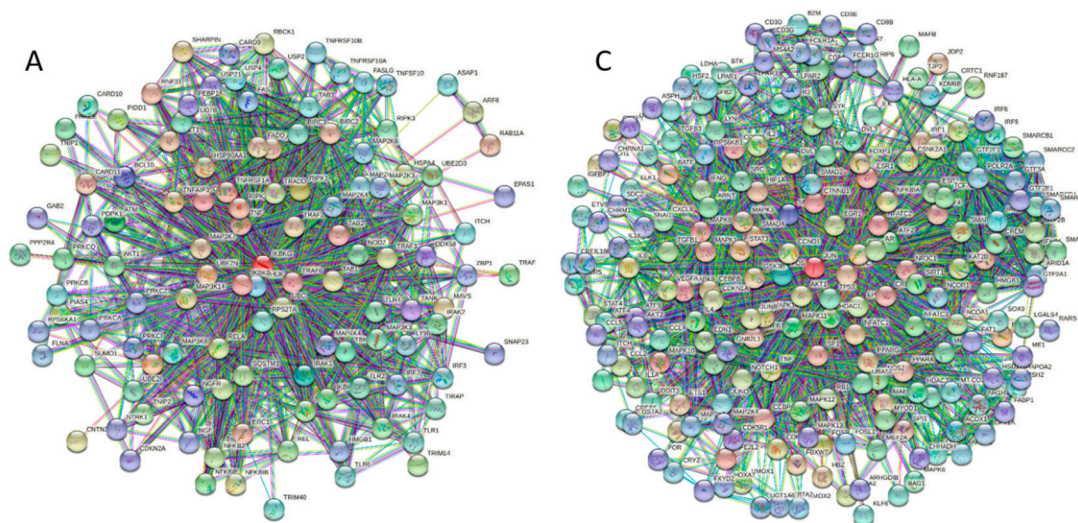


Figure 7. Cont.

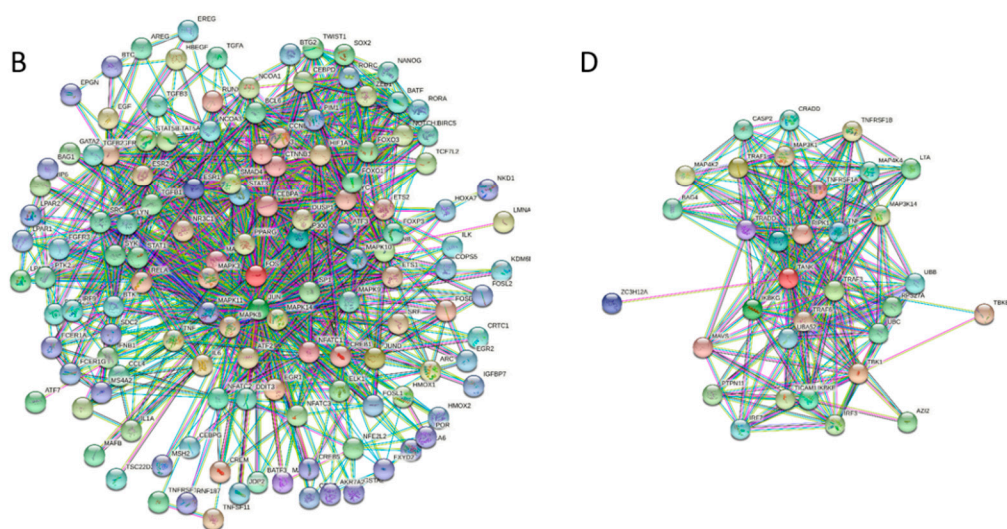


Figure 7. The PPI networks of human for IKK γ (A), c-FOS (B), Jun (C), and TANK (D) generated by STRING [98]. The IKK γ -centered PPI network includes 116 partners connected by 1209 interactions, indicating that each member of this network interacts with ~21 partners. c-FOS interacts with 131 proteins, each interacting with ~15 partners, thereby generating a network with 985 interactions. A total of 209 partners of Jun were linked to each other via 2076 interactions, being involved in ~20 interactions each. Finally, the TANK-centered PPI network included 52 partners connected by 320 interactions, indicating that each member of this network interacts with 12 partners.

In fact, C-FOS and Jun are mostly disordered, with each showing a long α -helix related to the formation of the coiled-coil structure in the C-FOS-Jun complex. IKK γ is predicted to have a V-shaped structure with two very long α -helices, whereas TANK, also being highly disordered, is expected to have two disjointed α -helices. Note that none of these proteins have a hydrophobic core, and therefore their long α -helices are unlikely to be stable in the unbound state. Figure 6 represents the functional disorder profiles of human IKK γ , c-FOS, Jun, and TANK generated by the D²P² platform [143] and shows that these four proteins are massively disordered and densely decorated by multiple various PTMs. Furthermore, they include numerous molecular recognition features (i.e., intrinsically disordered regions that are expected to undergo disorder-to-order transitions at the interaction with specific binding partners). Such features are commonly found within the IDRs of many proteins, where they were shown to play crucial roles in protein–protein interactions, potentially initiating early steps in molecular recognition [47,48]. IKK γ , c-FOS, Jun, and TANK have 6, 8, 8, and 9 MoRFs that cover 15.75%, 29.21%, 48.04%, and 22.35% of their entire sequences, respectively, indicating that very significant parts of these proteins are involved in molecular recognition.

Furthermore, MoRFs predicted in c-FOS (residues 180–212) and Jun (residues 241–250/252–284) overlap with the long helical segments predicted in these proteins by AlphaFold (residues 134–203 in c-FOS and 247–317). Similarly, two long helical segments of TANK (residues 5–69 and 130–165) included the predicted NoRFs (residues 12–21/54–65 and 142–159). These observations suggest that the indicated MoRFs can potentially adopt an α -helical structure at binding to their partners.

The fact that significant parts of these four proteins are predicted to be engaged in molecular recognition and undergo binding-induced disorder-to-order transition is further supported by Figure 7, which shows dense PPIs predicted for these four proteins by STRING. Each of these proteins represents a highly connected hub, indicating the heavy use of intrinsic disorder for PPIs. This is in line with previous studies that showed that intrinsic disorder is crucial for the functionality of hubs [52,159–164].

It should be noted that these four proteins are not an exception, and all other participants of TLR signaling analyzed in this study contain multiple MoRFs and act as hubs in densely packed PPI networks (see the Supplementary Figure S1 for this information).

To conclude this section, Figure 8 schematically represents the TLR-related signaling pathways [20,86,165]. Except for TLR3, which exclusively uses TRIF (Toll/IL-1 receptor domain-containing adaptor inducing IFN- β ; PPIDR = 66.29%) as a mediator of downstream signaling, the downstream signaling pathways of all other TLRs are mediated by the TIR domain-containing adaptor MyD88 (myeloid differentiation factor, also known as TIR domain-containing adaptor protein TIRAP, PPIDR = 19.93%). TLR4 may initiate both the MyD88-dependent and MyD88-independent pathways. The activation of TLR7/TLR8, TLR9, TLR10, and TLR10/TLR2 leads to the direct binding of their TIR domains to the MyD88 TIR domain. On the other hand, interaction of the TLR1/TLR2, TLR2/TLR6, and TLR4 with MyD88 is bridged by the junction protein MAL (MyD88 adapter-like, PPIDR = 42.53%) [166,167].

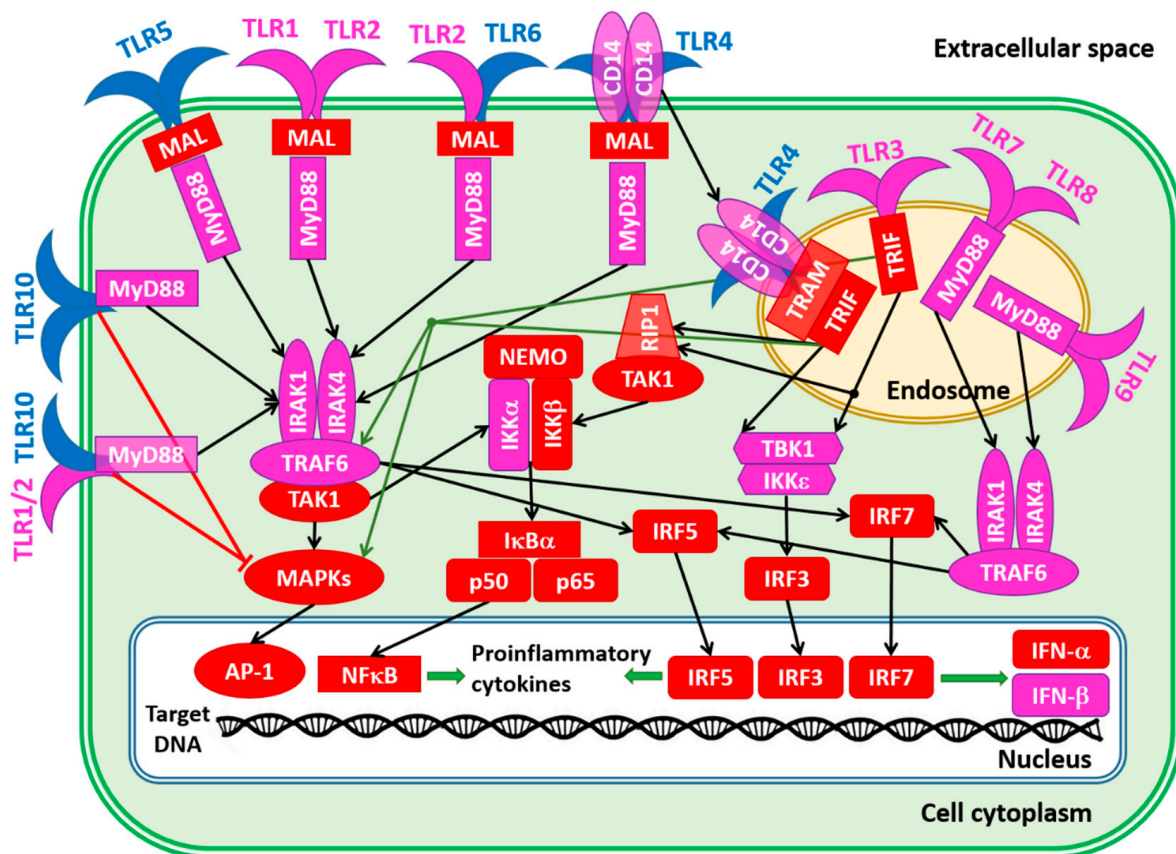


Figure 8. A schematic representation of the TLRs and related signaling networks.

MyD88 binding to the activated TLRs directly or via MAL initiates the MyD88-dependent downstream signaling pathways [166,167]. Here, MyD88 interacts and activates the IL-1 receptor-associated kinases IRAK1 (PPIDR = 52.67%) or IRAK4 (PPIDR = 33.48%). Activated IRAKs form a complex with TRAF6 (tumor necrosis factor (TNF) receptor-associated family 6, PPIDR = 23.37%). This leads to the activation of TAK1 (transformation growth factor- β (TGF- β)-activated kinase, PPIDR = 57.10%), which activates the IKK α /IKK β /IKK γ complex (inhibitors of nuclear factor- κ B (NF- κ B) kinase α , β , and γ , PPIDR = 24.56%, 35.45%, and 98.57%, respectively) and MAPKs (mitogen-activated protein kinases 1–15, whose PPIDR values range from 13.89% in MAPK14 to 63.24% in MAPK7).

Note that MAPK8, MAPK9, and MAPK10 are also known as c-Jun N-terminal kinases 1, 2, and 3, JNK1, JNK2, and JNK3 with PPIDs of 27.63%, 27.36%, and 26.72%.

MAPK3 (PPIDR = 22.95%) and MAPK1 (PPIDR = 16.67%) are also known as extracellular signal-regulated kinases 1 and 2 (ERK1 and ERK2), respectively. Finally, MAPK11 (p38-beta; PPIDR = 21.15%), MAPK12 (p38-gamma; PPIDR = 24.52%), MAPK13 (p38-delta; PPIDR = 30.68%), and MAPK14 (p38-beta; PPIDR = 13.89%) represent four p38 MAPKs that play important roles in the cascades of cellular responses evoked by extracellular stimuli. Activated MAPKs trigger the nuclear translocation of the activated protein-1 (AP-1) complex containing c-Jun (PPIDR = 82.78%) and c-FOS (PPIDR = 83.42%). The IKK α /IKK β complex releases the NF-kappa-B inhibitor alpha (I κ Ba, PPIDR = 39.75%) from the NF- κ B (a complex containing subunits p65 and p50 with PPIDRs of 64.61% and 33.16%, respectively) and triggers its nuclear translocation. In the nucleus, AP-1 and NF- κ B initiate biosynthesis of the proinflammatory cytokines [166,167]. Alternatively, activated TRAF6 can trigger the IRF5 (interferon regulatory factor 5; PPIDR = 43.17%) pathway, leading to the nuclear internalization of this factor, where it activates the expression of type I interferons (IFNs) IFNA (PPIDR = 31.75%) and INFB (PPIDR = 11.76%) and inflammatory cytokines [168–172].

TL3 and TL4 can initiate MyD88-independent downstream signaling pathways, with TLR4 being the only TLR that can trigger both MyD88-dependent and -independent pathways. In the MyD88-independent pathway, TLR4 complexed with CD14 (cluster of differentiation 14; PPIDR = 25.87%), which is a high affinity, horse shoe-shaped, glycosylphosphatidylinositol-(GPI-) anchored membrane protein and is internalized into the endosomes, where TRIF-related adaptor molecule (TRAM; PPIDR = 50.21%) binds to TLR4 and ensures the recruitment of TIR domain-containing adaptor-inducing interferon- β (TRIF; PPIDR = 66.29%) to TLR4 [173,174]. Then, TRAF family member-associated NF- κ B activator, (TANK-binding kinase-1 (TBK-1; PPIDR = 10.62%) and the inhibitor of nuclear factor- κ B (NF- κ B) kinase subunit epsilon (IKK ϵ ; PPIDR = 23.88%) are activated, leading to the phosphorylation and activation of interferon regulatory factor 3 (IRF3; PPIDR = 37.94%), which enters the nucleus and initiates the transcription of anti-inflammatory cytokines [175]. Furthermore, in this pathway, TRIF can activate NF- κ B and promote its nuclear translocation through receptor-interacting protein 1 (RIP1; PPIDR = 47.84%) and transformation growth factor- β (TGF- β)-activated kinase (TAK1; PPIDR = 57.10%) or TRAF6 [176]. It can also act via the activation of MAPKs to induce AP-1, thereby triggering a proinflammatory response [177].

The internalization of viral PAMPs leads to the activation of the TLR3, TLR7/8, and TLR9 in the endosomes. The activation of TLR3 is associated with the initiation of the MyD88-independent pathways. Similar to TLR4, TLR3 interacts with TRIF, and this leads to the IKK ϵ /TBK-1-driven activation of IRF3. Although TLR7, TLR8, and TLR9 are on the MyD88-dependent pathway, MAL is not needed for their interaction with MyD88. After MyD88 binding, they activate IRAKs that bind to TRAF6, leading to IRF5 and IRF7 (PPIDR = 58.08%) activation and translocation to the nucleus, where these interferon regulatory factors trigger the transcription of anti-inflammatory cytokines.

Finally, the role of TLR10 also needs to be addressed, which, despite being discovered in 2001 [178], is considered to be an orphan receptor whose ligands and functions are poorly known [86,179,180]. Although this receptor can homodimerize and form heterodimers with TLR1, TLR2, and TLR6 [181–184], the functional significance of the resulting complexes and TLR10 itself remains mostly unknown [182]. It was shown that the TLR10/TLR2 heterodimer and TLR10/TLR10 can bind MyD88, but they are incapable of NF- κ B activation [185]. It seems that TLR10 serves as an inhibitor of the MyD88 dependent and independent pathways [86,178].

The data presented in this section are summarized in Figure 8, showing the proteins involved in these TLR pathways as being colored based on their intrinsic disorder status, with highly ordered, moderately disordered, and highly disordered proteins being shown by the blue, pink, and red colors, respectively. With the exception of four TLRs (TLR4, TLR5, TLR6, and TLR10), all the proteins in these networks were either moderately or highly disordered. This once again emphasizes the importance of intrinsic disorder for the regulation and control of these crucial pathways.

4. TLRs in HCV Infection

Although host cells contain several pattern recognition receptors that can recognize HCV such as C-type lectin receptors (CLRs), cytosolic DNA sensors (CDs), NOD-like receptors (NLRs), RIG-I-like receptors (RLRs), and Toll-like receptors (TLRs) [36], TLRs deserve special attention due to their capability to rapidly establish antiviral response and serve as important players in the process of HCV infection [20]. This is because TLRs can recognize several viral PAMPs and efficiently bind to various HCV structures [20]. A detailed description of the roles of HCV proteins in altering and modulating the TLR-based responses can be found elsewhere [20]. The section below provides a brief overview of this phenomenon from the angle of intrinsic disorder.

Figure 9 shows that half of the HCV proteins is tightly related to the TLRs. For example, interactions of the HCV core (PPIDR = 68.18%), NS3 (PPIDR = 22.03%), and NS5A (PPIDR = 47.99%) proteins with TLR1/TLR2 and TLR2/TLR6 activate the downstream TLR2-specific signaling processes in the MyD88-dependent manner (see Figure 8). Here, the TLR2-specific intracellular pathway is utilized by the HCV core and NS3 proteins to activate innate immune and inflammatory cells [186]. Both HCV core and NS3 proteins can be recognized by the TLR2/TLR1 and TLR2/TLR6 heterodimers [187]. Importantly, in chronic HCV infection, the HCV-triggered activation of NF- κ B (a complex containing subunits p65 and p50 with PPIDRs of 64.61% and 33.16%, respectively) and AP-1 (a complex of c-Jun (PPIDR = 82.78%) and c-FOS (PPIDR = 83.42%)) transcription factors, and the phosphorylation of JNKs (JNK1, JNK2, and JNK3 with PPIDs of 27.63%, 27.36%, and 26.72%) via the MyD88-driven recruitment of IRAK1 (PPIDR = 52.67%), IRAK4 (PPIDR = 33.48%), and TRAF6 (PPIDR = 22.37%) is believed to be linked to hepatocyte damage, as both hepatocyte metabolism and inflammation/injury/fibrosis are related to the TLR-activated JNKs [188,189].

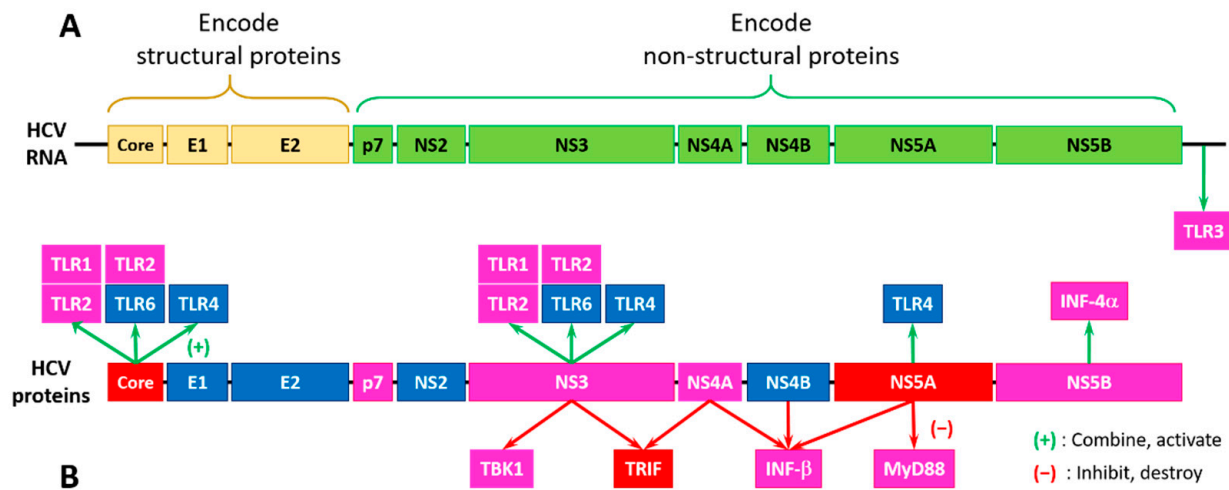


Figure 9. The organization of the HCV genome (A) and effects of the HCV-encoded proteins on Toll-like receptors (TLRs) and related downstream molecules (B). Proteins are colored based on their intrinsic disorder status, where highly disordered, moderately disordered, and highly ordered proteins are shown by red, pink, and blue colors, respectively. Proteins are classified based on the accepted strategy rooted in the percent of predicted intrinsic disorder (PPIDR) of query proteins, where proteins are considered as highly ordered, moderately disordered, and highly disordered, if their PPIDR <10%, 10% \leq PPIDR < 30%, and PPIDR \geq 30%, respectively [190].

As was discussed above, TLR4 can activate downstream pathways both in the MyD88-dependent and MyD88-independent manner. Although TLR4 activation is typically induced by the lipopolysaccharides (LPSs), HCV NS5A can bind to TLR4 directly, without LPS stimulation, thereby promoting the MyD88-independent activation of the downstream

molecules through the pathways related to TRIF (PPIDR = 66.29%) (see Figure 8). This NS5A-TLR4 binding on monocytes leads to an imbalance of inflammatory cytokines enhancing the IL-10 production and decreasing the IL-12 production [191]. This inflammatory cytokine imbalance inhibits the virus-killing effect of the natural killer (NK) cells, thereby helping HCV to evade immune surveillance [191]. Furthermore, NS5A was shown to upregulate the TLR4 expression in the peripheral blood mononuclear cells and B cells, leading to the enhanced production of IFN- β and IL-6 [192]. On the other hand, in hepatocytes, HCV NS5A was shown to downregulate TLR4 expression, thereby inhibiting the LPS-mediated apoptosis of hepatocytes [193].

In addition to the effects associated with the activation of TLRs by HCV proteins, NS3 and NS4A proteins can interact with the downstream molecules TBK1 (PPIDR = 10.62%) and TRIF (PPIDR = 66.29%), thereby distorting the TLR3-based MyD88-independent pathways, leading to the initiation of the IFN production. Here, the TLR3 adaptor protein TRIF is proteolytically degraded by HCV NS3/NS4A, which impairs the IRF3 (PPIDR = 37.94%)-induced production of IFN, whereas the direct NS3 binding to TBK1 damages the activation of IRF3 and upregulation of IFN- β (PPIDR = 11.76%) [20,194,195]. It was also shown that the IFN- β production can be promoted by NS5B (PPIDR = 15.40%), which may synthesize a nonspecific double-stranded RNA (dsRNA) as a TLR3 ligand, whereas the activities of NS4A (PPIDR = 18.52%), NS4B (PPIDR = 9.20%), and NS5A (PPIDR = 47.99%) can inhibit this pathway by altering the dsRNA synthesis or distorting the TLR3-dsRNA recognition [196].

TLR7/8 can be activated by the HCV single-stranded RNA. It was shown that in the peripheral blood monocytes of the HCV-infected patients, the TLR7 expression was noticeably reduced due to the TLR7 gene distortion and instability of the TLR7 mRNA [197]. Furthermore, NS5A can inhibit the production of some inflammatory factors by binding to the MyD88 death domain, thereby suppressing TLR7/8 signaling [198,199] and affecting other MyD88-dependent pathways downstream of TLRs [20].

Finally, since TLR9 can only bind to DNA, the HCV single-stranded RNA cannot activate this receptor [200]. However, TLR9 can still affect HCV infection via apoptotic cell DNA [201]. Furthermore, similar to TLR7, the levels of the TLR9 mRNA and protein are downregulated in the peripheral blood mononuclear cells from HCV infected patients, being negatively correlated with serum viral copies [202].

5. Conclusions

In this article, we analyzed the prevalence and potential functional roles of intrinsic disorder in HCV proteins, TLRs, and some major players of the TLR-induced downstream pathways. To the best of our knowledge, this work, being a compilation of the state-of-the-art and common knowledge on HCV infection and pathophysiological conditions, represents a first systematic study of the intrinsic disorder-based interplay between HCV, TLRs, and TLR-induced downstream pathways. We confirmed that HCV contains four ordered proteins (E1, E2, NS2, and NS4B), five moderately disordered proteins (p7, NS3, NS4A, and NS5B), and two highly disordered proteins (core and NS5A). We also showed that based on their intrinsic disorder content, human TLRs can be arranged as follows: TLR5 < TLR6 < TLR10 < TLR4 < TLR9 < TLR1 < TLR7 < TLR3 < TLR2 < TLR8. The first four TLRs in this list are expected to be mostly ordered, whereas the remaining six TLRs were predicted as moderately disordered. Analysis of the 41 TLR signaling-related proteins revealed that they contained high levels of intrinsic disorder that ranged from 10.62% in TBK1 to 98.75% in IKK γ (NEMO). Of these proteins, 13 are expected to have more than 50% disordered residues, 16 proteins possess PPIDR values between 25% and 50%, and the remaining 12 proteins have disorder content that ranges from 10.62% (TBK1) to 24.56% (IKK α). In all HCV, TLRs, and TLR signaling proteins analyzed in this study, disordered residues are assembled into the functional IDRs, which serve either as a signal for a variety of posttranslational modifications or are used for protein–protein interactions, often being capable of undergoing the binding-induced folding at interaction with specific partners.

The fact that most of these proteins have intrinsic disorder, are capable of undergoing functional disorder-to-order transitions, and can be subjected to multiple PTMs indicates that each of them, despite being encoded by a single gene, exists as a dynamic ensemble of structurally and functionally distinct protein molecules, known as proteoforms [65,203]. Therefore, the functionality of these proteins can be described within the frames of the “protein structure–function continuum” model, where the structure of a protein represents a highly dynamic conformational ensemble containing multiple proteoforms that have different structural features and might have various functions [204–206]. Such disorder-based structural and functional heterogeneity of HCV proteins, TLRs, and proteins from the TLR pathways are important for a better understanding of both the HCV pathogenesis and the innate immune response to the HCV infection.

These observations are in line with the well-known association between the protein intrinsic disorder and pathogenesis of various human diseases [81,207–212]. They also agree with the results of the comprehensive bioinformatics analyses of the prevalence of protein intrinsic disorder in various viruses such as human papillomaviruses (HPVs) [213], HCV [41], influenza viruses [214], HIV-1 [215], Dengue virus [216], respiratory syncytial virus (RSV) [217], Zika virus [218,219], Chikungunya virus [220,221], rotavirus [222], Japanese encephalitis virus [223], SARS-CoV-2 [224,225], human SARS and bat SARS-like coronaviruses [224], Middle East respiratory syndrome MERS coronavirus [226,227], and Chandipura virus [228] as well as in the interactomes of HPV [229] and HCV [40]. They are also supported by the results of the evaluation of intrinsic disorder in proteins involved in innate anti-viral immunity [230] and the comprehensive bioinformatics analysis of the global prevalence of intrinsic disorder in 6108 viral proteomes [231]. Our study emphasizes the importance of the systematic analysis of intrinsic disorder for a better understanding of the pathogenesis of viral infections. Furthermore, this work provides important information that can be utilized in the future development of the novel therapy against HCV hepatitis.

Supplementary Materials: The following supporting information can be downloaded at: <https://www.mdpi.com/article/10.3390/biology11071091/s1>, Figure S1: Amino acid sequences, structural and intrinsic disorder-based features of HCV proteins, human TLRs, and major players of the TLR-regulated downstream signaling pathways; Table S1: Some physico-chemical and intrinsic disorder-related features of HCV proteins, human TLRs, and major players of the TLR-regulated downstream signaling pathways.

Author Contributions: Conceptualization, V.N.U.; Literature analysis, E.M.R., A.A.A. and V.N.U.; Validation, E.M.R., A.A.A. and V.N.U.; Investigation, V.N.U.; Data curation, E.M.R., A.A.A. and V.N.U.; Writing—original draft preparation, V.N.U.; Writing—review and editing, E.M.R., A.A.A. and V.N.U.; Visualization, V.N.U.; Supervision, V.N.U.; Project administration, V.N.U.; Funding acquisition, E.M.R. All authors have read and agreed to the published version of the manuscript.

Funding: The authors extend their appreciation to the Deputyship for Research & Innovation, Ministry of Education in Saudi Arabia, for funding this research work through project number 838.

Institutional Review Board Statement: Not applicable.

Informed Consent Statement: Not applicable.

Data Availability Statement: The data presented in this study are available in this article and in the Supplementary Materials.

Conflicts of Interest: The authors declare no conflict of interest. The funders had no role in the design of the study; in the collection, analyses, or interpretation of data; in the writing of the manuscript, or in the decision to publish the results.

References

1. Stapleton, J.T.; Fong, S.; Muerhoff, A.S.; Bukh, J.; Simmonds, P. The GB viruses: A review and proposed classification of GBV-A, GBV-C (HGV), and GBV-D in genus Pegivirus within the family Flaviviridae. *J. Gen. Virol.* **2011**, *92*, 233–246. [CrossRef] [PubMed]

2. Deinhardt, F.; Holmes, A.W.; Capps, R.B.; Popper, H. Studies on the transmission of human viral hepatitis to marmoset monkeys. I. Transmission of disease, serial passages, and description of liver lesions. *J. Exp. Med.* **1967**, *125*, 673–688. [[CrossRef](#)] [[PubMed](#)]
3. Rosen, H.R. Clinical practice. Chronic hepatitis C infection. *N. Engl. J. Med.* **2011**, *364*, 2429–2438. [[CrossRef](#)] [[PubMed](#)]
4. Maheshwari, A.; Thuluvath, P.J. Management of acute hepatitis C. *Clin. Liver Dis.* **2010**, *14*, 169–176. [[CrossRef](#)]
5. WHO. World Health Organization: Hepatitis C. Available online: <https://www.who.int/en/news-room/fact-sheets/detail/hepatitis-c> (accessed on 19 May 2022).
6. Lanini, S.; Easterbrook, P.J.; Zumla, A.; Ippolito, G. Hepatitis C: Global epidemiology and strategies for control. *Clin. Microbiol. Infect.* **2016**, *22*, 833–838. [[CrossRef](#)]
7. Global Burden of Disease Study 2013 Collaborators. Global, regional, and national incidence, prevalence, and years lived with disability for 301 acute and chronic diseases and injuries in 188 countries, 1990–2013: A systematic analysis for the Global Burden of Disease Study 2013. *Lancet* **2015**, *386*, 743–800. [[CrossRef](#)]
8. Lozano, R.; Naghavi, M.; Foreman, K.; Lim, S.; Shibuya, K.; Aboyans, V.; Abraham, J.; Adair, T.; Aggarwal, R.; Ahn, S.Y.; et al. Global and regional mortality from 235 causes of death for 20 age groups in 1990 and 2010: A systematic analysis for the Global Burden of Disease Study 2010. *Lancet* **2012**, *380*, 2095–2128. [[CrossRef](#)]
9. Petruzzello, A.; Marigliano, S.; Loquercio, G.; Cozzolino, A.; Cacciapuoti, C. Global epidemiology of hepatitis C virus infection: An up-date of the distribution and circulation of hepatitis C virus genotypes. *World J. Gastroenterol.* **2016**, *22*, 7824–7840. [[CrossRef](#)]
10. Gower, E.; Estes, C.; Blach, S.; Razavi-Shearer, K.; Razavi, H. Global epidemiology and genotype distribution of the hepatitis C virus infection. *J. Hepatol.* **2014**, *61*, S45–S57. [[CrossRef](#)]
11. Mohd Hanafiah, K.; Groeger, J.; Flaxman, A.D.; Wiersma, S.T. Global epidemiology of hepatitis C virus infection: New estimates of age-specific antibody to HCV seroprevalence. *Hepatology* **2013**, *57*, 1333–1342. [[CrossRef](#)]
12. Gravitz, L. Introduction: A smouldering public-health crisis. *Nature* **2011**, *474*, S2–S4. [[CrossRef](#)]
13. Riou, J.; Ait Ahmed, M.; Blake, A.; Vozlinsky, S.; Brichtler, S.; Eholie, S.; Boelle, P.Y.; Fontanet, A.; Thursz, M.; HCV Epidemiology in Africa Group. Hepatitis C virus seroprevalence in adults in Africa: A systematic review and meta-analysis. *J. Viral. Hepat.* **2016**, *23*, 244–255. [[CrossRef](#)]
14. Njouom, R.; Caron, M.; Besson, G.; Ndong-Atome, G.R.; Makuwa, M.; Pouillot, R.; Nkoghe, D.; Leroy, E.; Kazanji, M. Phylogeography, risk factors and genetic history of hepatitis C virus in Gabon, central Africa. *PLoS ONE* **2012**, *7*, e42002. [[CrossRef](#)]
15. Sharvadze, L.; Nelson, K.E.; Imnadze, P.; Karchava, M.; Tsertsvadze, T. Prevalence of HCV and genotypes distribution in general population of Georgia. *Georgian Med. News* **2008**, *165*, 71–77.
16. Saraswat, V.; Norris, S.; de Knegt, R.J.; Sanchez Avila, J.F.; Sonderup, M.; Zuckerman, E.; Arkkila, P.; Stedman, C.; Acharya, S.; Aho, I.; et al. Historical epidemiology of hepatitis C virus (HCV) in select countries—Volume 2. *J. Viral. Hepat.* **2015**, *22* (Suppl. S1), 6–25. [[CrossRef](#)]
17. Tserenpuntsag, B.; Nelson, K.; Lamjav, O.; Triner, W.; Smith, P.; Kacica, M.; McNutt, L.A. Prevalence of and risk factors for hepatitis B and C infection among Mongolian blood donors. *Transfusion* **2010**, *50*, 92–99. [[CrossRef](#)]
18. Umer, M.; Iqbal, M. Hepatitis C virus prevalence and genotype distribution in Pakistan: Comprehensive review of recent data. *World J. Gastroenterol.* **2016**, *22*, 1684–1700. [[CrossRef](#)]
19. Ansari, M.A.; Aranday-Cortes, E.; Ip, C.L.; da Silva Filipe, A.; Lau, S.H.; Bamford, C.; Bonsall, D.; Trebes, A.; Piazza, P.; Sreenu, V.; et al. Interferon lambda 4 impacts the genetic diversity of hepatitis C virus. *Elife* **2019**, *8*, 42463. [[CrossRef](#)]
20. Gao, Y.; Nepal, N.; Jin, S.Z. Toll-like receptors and hepatitis C virus infection. *Hepatobiliary Pancreat. Dis. Int.* **2021**, *20*, 521–529. [[CrossRef](#)]
21. Smith, D.B.; Bukh, J.; Kuiken, C.; Muerhoff, A.S.; Rice, C.M.; Stapleton, J.T.; Simmonds, P. Expanded classification of hepatitis C virus into 7 genotypes and 67 subtypes: Updated criteria and genotype assignment web resource. *Hepatology* **2014**, *59*, 318–327. [[CrossRef](#)]
22. Simmonds, P.; Holmes, E.C.; Cha, T.A.; Chan, S.W.; McOmish, F.; Irvine, B.; Beall, E.; Yap, P.L.; Kolberg, J.; Urdea, M.S. Classification of hepatitis C virus into six major genotypes and a series of subtypes by phylogenetic analysis of the NS-5 region. *J. Gen. Virol.* **1993**, *74 Pt 11*, 2391–2399. [[CrossRef](#)]
23. Palladino, C.; Ezeonwumelu, I.J.; Marcelino, R.; Briz, V.; Moranguinho, I.; Serejo, F.; Velosa, J.F.; Marinho, R.T.; Borrego, P.; Taveira, N. Epidemic history of hepatitis C virus genotypes and subtypes in Portugal. *Sci. Rep.* **2018**, *8*, 12266. [[CrossRef](#)]
24. Wilkins, T.; Malcolm, J.K.; Raina, D.; Schade, R.R. Hepatitis C: Diagnosis and treatment. *Am. Fam. Physician* **2010**, *81*, 1351–1357.
25. Nakano, T.; Lau, G.M.; Lau, G.M.; Sugiyama, M.; Mizokami, M. An updated analysis of hepatitis C virus genotypes and subtypes based on the complete coding region. *Liver Int. Off. J. Int. Assoc. Study Liver* **2012**, *32*, 339–345. [[CrossRef](#)]
26. Inamullah, Idrees, M.; Ahmed, H.; Sajid ul, g.; Ali, M.; Ali, L.; Ahmed, A. Hepatitis C virus genotypes circulating in district Swat of Khyber Pakhtoonkhaw, Pakistan. *Virol. J.* **2011**, *8*, 16. [[CrossRef](#)]
27. Cha, T.A.; Kolberg, J.; Irvine, B.; Stempien, M.; Beall, E.; Yano, M.; Choo, Q.L.; Houghton, M.; Kuo, G.; Han, J.H.; et al. Use of a signature nucleotide sequence of hepatitis C virus for detection of viral RNA in human serum and plasma. *J. Clin. Microbiol.* **1991**, *29*, 2528–2534. [[CrossRef](#)]
28. Tokita, H.; Shrestha, S.M.; Okamoto, H.; Sakamoto, M.; Horikita, M.; Iizuka, H.; Shrestha, S.; Miyakawa, Y.; Mayumi, M. Hepatitis C virus variants from Nepal with novel genotypes and their classification into the third major group. *J. Gen. Virol.* **1994**, *75 Pt 4*, 931–936. [[CrossRef](#)]

29. Gouvea, V.; Snellings, N.; Cohen, S.J.; Warren, R.L.; Myint, K.S.; Shrestha, M.P.; Vaughn, D.W.; Hoke, C.H., Jr.; Innis, B.L. Hepatitis E virus in Nepal: Similarities with the Burmese and Indian variants. *Virus Res.* **1997**, *52*, 87–96. [[CrossRef](#)]
30. Tokita, H.; Okamoto, H.; Iizuka, H.; Kishimoto, J.; Tsuda, F.; Lesmana, L.A.; Miyakawa, Y.; Mayumi, M. Hepatitis C virus variants from Jakarta, Indonesia classifiable into novel genotypes in the second (2e and 2f), tenth (10a) and eleventh (11a) genetic groups. *J. Gen. Virol.* **1996**, *77 Pt 2*, 293–301. [[CrossRef](#)]
31. Takada, N.; Takase, S.; Takada, A.; Date, T. Differences in the hepatitis C virus genotypes in different countries. *J. Hepatol.* **1993**, *17*, 277–283. [[CrossRef](#)]
32. McOmish, F.; Yap, P.L.; Dow, B.C.; Follett, E.A.; Seed, C.; Keller, A.J.; Cobain, T.J.; Krusius, T.; Kolho, E.; Naukkarinen, R.; et al. Geographical distribution of hepatitis C virus genotypes in blood donors: An international collaborative survey. *J. Clin. Microbiol.* **1994**, *32*, 884–892. [[CrossRef](#)] [[PubMed](#)]
33. Noursbaum, J.B.; Pol, S.; Nalpas, B.; Landais, P.; Berthelot, P.; Brechot, C. Hepatitis C virus type 1b (II) infection in France and Italy. Collaborative Study Group. *Ann. Intern. Med.* **1995**, *122*, 161–168. [[CrossRef](#)] [[PubMed](#)]
34. Zein, N.N.; Rakela, J.; Krawitt, E.L.; Reddy, K.R.; Tominaga, T.; Persing, D.H. Hepatitis C virus genotypes in the United States: Epidemiology, pathogenicity, and response to interferon therapy. Collaborative Study Group. *Ann. Intern. Med.* **1996**, *125*, 634–639. [[CrossRef](#)] [[PubMed](#)]
35. Dusheiko, G.; Schmilovitz-Weiss, H.; Brown, D.; McOmish, F.; Yap, P.L.; Sherlock, S.; McIntyre, N.; Simmonds, P. Hepatitis C virus genotypes: An investigation of type-specific differences in geographic origin and disease. *Hepatology* **1994**, *19*, 13–18. [[CrossRef](#)]
36. Sepulveda-Crespo, D.; Resino, S.; Martinez, I. Innate Immune Response against Hepatitis C Virus: Targets for Vaccine Adjuvants. *Vaccines* **2020**, *8*, 313. [[CrossRef](#)]
37. Kato, N. Genome of human hepatitis C virus (HCV): Gene organization, sequence diversity, and variation. *Microb. Comp. Genom.* **2000**, *5*, 129–151. [[CrossRef](#)]
38. Dubuisson, J. Hepatitis C virus proteins. *World J. Gastroenterol.* **2007**, *13*, 2406–2415. [[CrossRef](#)]
39. Reed, K.E.; Rice, C.M. Overview of hepatitis C virus genome structure, polyprotein processing, and protein properties. *Curr. Top. Microbiol. Immunol.* **2000**, *242*, 55–84. [[CrossRef](#)]
40. Dolan, P.T.; Roth, A.P.; Xue, B.; Sun, R.; Dunker, A.K.; Uversky, V.N.; LaCount, D.J. Intrinsic disorder mediates hepatitis C virus core-host cell protein interactions. *Protein Sci.* **2015**, *24*, 221–235. [[CrossRef](#)]
41. Fan, X.; Xue, B.; Dolan, P.T.; LaCount, D.J.; Kurgan, L.; Uversky, V.N. The intrinsic disorder status of the human hepatitis C virus proteome. *Mol. Biosyst.* **2014**, *10*, 1345–1363. [[CrossRef](#)]
42. Tokuriki, N.; Oldfield, C.J.; Uversky, V.N.; Berezovsky, I.N.; Tawfik, D.S. Do viral proteins possess unique biophysical features? *Trends Biochem. Sci.* **2009**, *34*, 53–59. [[CrossRef](#)]
43. Berezovsky, I.N. The diversity of physical forces and mechanisms in intermolecular interactions. *Phys. Biol.* **2011**, *8*, 035002. [[CrossRef](#)]
44. Xue, B.; Williams, R.W.; Oldfield, C.J.; Goh, G.K.; Dunker, A.K.; Uversky, V.N. Viral disorder or disordered viruses: Do viral proteins possess unique features? *Protein Pept. Lett.* **2010**, *17*, 932–951. [[CrossRef](#)]
45. Dunker, A.K.; Lawson, J.D.; Brown, C.J.; Williams, R.M.; Romero, P.; Oh, J.S.; Oldfield, C.J.; Campen, A.M.; Ratliff, C.M.; Higgs, K.W.; et al. Intrinsically disordered protein. *J. Mol. Graph Model* **2001**, *19*, 26–59. [[CrossRef](#)]
46. Dunker, A.K.; Obradovic, Z.; Romero, P.; Garner, E.C.; Brown, C.J. Intrinsic protein disorder in complete genomes. *Genome Inf. Ser. Workshop Genome Inf.* **2000**, *11*, 161–171.
47. Tompa, P. Intrinsically unstructured proteins. *Trends Biochem. Sci.* **2002**, *27*, 527–533. [[CrossRef](#)]
48. Uversky, V.N. Natively unfolded proteins: A point where biology waits for physics. *Protein Sci.* **2002**, *11*, 739–756. [[CrossRef](#)]
49. Uversky, V.N. The mysterious unfoldome: Structureless, underappreciated, yet vital part of any given proteome. *J. Biomed. Biotechnol.* **2010**, *2010*, 568068. [[CrossRef](#)]
50. Uversky, V.N.; Dunker, A.K. Understanding protein non-folding. *Biochim. Biophys. Acta* **2010**, *1804*, 1231–1264. [[CrossRef](#)]
51. Uversky, V.N.; Gillespie, J.R.; Fink, A.L. Why are “natively unfolded” proteins unstructured under physiologic conditions? *Proteins* **2000**, *41*, 415–427. [[CrossRef](#)]
52. Dunker, A.K.; Cortese, M.S.; Romero, P.; Iakoucheva, L.M.; Uversky, V.N. Flexible nets. The roles of intrinsic disorder in protein interaction networks. *FEBS J.* **2005**, *272*, 5129–5148. [[CrossRef](#)] [[PubMed](#)]
53. Ward, J.J.; Sodhi, J.S.; McGuffin, L.J.; Buxton, B.F.; Jones, D.T. Prediction and functional analysis of native disorder in proteins from the three kingdoms of life. *J. Mol. Biol.* **2004**, *337*, 635–645. [[CrossRef](#)] [[PubMed](#)]
54. Kwofie, S.K.; Schaefer, U.; Sundararajan, V.S.; Bajic, V.B.; Christoffels, A. HCVpro: Hepatitis C virus protein interaction database. *Infect. Genet. Evol. J. Mol. Epidemiol. Evol. Genet. Infect. Dis.* **2011**, *11*, 1971–1977. [[CrossRef](#)] [[PubMed](#)]
55. Dolan, P.T.; Zhang, C.-Y.; Khadka, S.; Arumugaswami, V.; Vangeloff, A.D.; Heaton, N.S.; Sahasrabudhe, S.; Randall, G.; Sun, R.; LaCount, D. Identification and Comparative Analysis of Hepatitis C Virus-Host Cell Protein Interactions. *Mol. Biosyst.* **2013**, *9*, 3199–3209. [[CrossRef](#)]
56. Germain, M.A.; Chatel-Chaix, L.; Gagne, B.; Bonneil, E.; Thibault, P.; Pradezynski, F.; de Chasse, B.; Meyniel-Shicklin, L.; Lotteau, V.; Baril, M.; et al. Elucidating Novel Hepatitis C Virus/Host Interactions Using Combined Mass Spectrometry and Functional Genomics Approaches. *Mol. Cell. Proteom. MCP* **2014**, *13*, 184–203. [[CrossRef](#)]
57. Dunker, A.K.; Garner, E.; Guillot, S.; Romero, P.; Albrecht, K.; Hart, J.; Obradovic, Z.; Kissinger, C.; Villafranca, J.E. Protein disorder and the evolution of molecular recognition: Theory, predictions and observations. *Pac. Symp. Biocomput.* **1998**, *3*, 473–484.

58. Wright, P.E.; Dyson, H.J. Intrinsically unstructured proteins: Re-assessing the protein structure-function paradigm. *J. Mol. Biol.* **1999**, *293*, 321–331. [[CrossRef](#)]
59. Daughdrill, G.W.; Pielak, G.J.; Uversky, V.N.; Cortese, M.S.; Dunker, A.K. Natively disordered proteins. In *Handbook of Protein Folding*; Buchner, J., Kiefhaber, T., Eds.; Wiley-VCH, Verlag GmbH & Co. KGaA: Weinheim, Germany, 2005; pp. 271–353.
60. Uversky, V.N. Unusual biophysics of intrinsically disordered proteins. *Biochim. Biophys. Acta* **2013**, *1834*, 932–951. [[CrossRef](#)]
61. Dunker, A.K.; Obradovic, Z. The protein trinity—Linking function and disorder. *Nat. Biotechnol.* **2001**, *19*, 805–806. [[CrossRef](#)]
62. Uversky, V.N. A decade and a half of protein intrinsic disorder: Biology still waits for physics. *Protein Sci.* **2013**, *22*, 693–724. [[CrossRef](#)]
63. Uversky, V.N. Intrinsic disorder-based protein interactions and their modulators. *Curr. Pharm. Des.* **2013**, *19*, 4191–4213. [[CrossRef](#)]
64. Jakob, U.; Kriwacki, R.; Uversky, V.N. Conditionally and transiently disordered proteins: Awakening cryptic disorder to regulate protein function. *Chem. Rev.* **2014**, *114*, 6779–6805. [[CrossRef](#)]
65. Uversky, V.N. p53 Proteoforms and Intrinsic Disorder: An Illustration of the Protein Structure-Function Continuum Concept. *Int. J. Mol. Sci.* **2016**, *17*, 1874. [[CrossRef](#)]
66. Uversky, V.N. Functional roles of transiently and intrinsically disordered regions within proteins. *FEBS J.* **2015**, *282*, 1182–1189. [[CrossRef](#)]
67. Iakoucheva, L.M.; Brown, C.J.; Lawson, J.D.; Obradovic, Z.; Dunker, A.K. Intrinsic disorder in cell-signaling and cancer-associated proteins. *J. Mol. Biol.* **2002**, *323*, 573–584. [[CrossRef](#)]
68. Dyson, H.J.; Wright, P.E. Intrinsically unstructured proteins and their functions. *Nat. Rev. Mol. Cell Biol.* **2005**, *6*, 197–208. [[CrossRef](#)]
69. Liu, J.; Perumal, N.B.; Oldfield, C.J.; Su, E.W.; Uversky, V.N.; Dunker, A.K. Intrinsic disorder in transcription factors. *Biochemistry* **2006**, *45*, 6873–6888. [[CrossRef](#)]
70. Minezaki, Y.; Homma, K.; Kinjo, A.R.; Nishikawa, K. Human transcription factors contain a high fraction of intrinsically disordered regions essential for transcriptional regulation. *J. Mol. Biol.* **2006**, *359*, 1137–1149. [[CrossRef](#)]
71. Xue, B.; Oldfield, C.J.; Van, Y.Y.; Dunker, A.K.; Uversky, V.N. Protein intrinsic disorder and induced pluripotent stem cells. *Mol. Biosyst.* **2012**, *8*, 134–150. [[CrossRef](#)]
72. Peysselon, F.; Xue, B.; Uversky, V.N.; Ricard-Blum, S. Intrinsic disorder of the extracellular matrix. *Mol. Biosyst.* **2011**, *7*, 3353–3365. [[CrossRef](#)]
73. Ito, M.; Tohsato, Y.; Sugisawa, H.; Kohara, S.; Fukuchi, S.; Nishikawa, I.; Nishikawa, K. Intrinsically disordered proteins in human mitochondria. *Genes Cells Devoted Mol. Cell. Mech.* **2012**, *17*, 817–825. [[CrossRef](#)] [[PubMed](#)]
74. Peng, Z.; Oldfield, C.J.; Xue, B.; Mizianty, M.J.; Dunker, A.K.; Kurgan, L.; Uversky, V.N. A creature with a hundred waggly tails: Intrinsically disordered proteins in the ribosome. *Cell. Mol. Life Sci. CMLS* **2014**, *71*, 1477–1504. [[CrossRef](#)] [[PubMed](#)]
75. Homma, K.; Fukuchi, S.; Nishikawa, K.; Sakamoto, S.; Sugawara, H. Intrinsically disordered regions have specific functions in mitochondrial and nuclear proteins. *Mol. Biosyst.* **2012**, *8*, 247–255. [[CrossRef](#)] [[PubMed](#)]
76. Peng, Z.; Mizianty, M.J.; Xue, B.; Kurgan, L.; Uversky, V.N. More than just tails: Intrinsic disorder in histone proteins. *Mol. Biosyst.* **2012**, *8*, 1886–1901. [[CrossRef](#)]
77. Tompa, P. The interplay between structure and function in intrinsically unstructured proteins. *FEBS Lett.* **2005**, *579*, 3346–3354. [[CrossRef](#)]
78. Radivojac, P.; Iakoucheva, L.M.; Oldfield, C.J.; Obradovic, Z.; Uversky, V.N.; Dunker, A.K. Intrinsic disorder and functional proteomics. *Biophys. J.* **2007**, *92*, 1439–1456. [[CrossRef](#)]
79. Xie, H.; Vucetic, S.; Iakoucheva, L.M.; Oldfield, C.J.; Dunker, A.K.; Obradovic, Z.; Uversky, V.N. Functional anthology of intrinsic disorder. 3. Ligands, post-translational modifications, and diseases associated with intrinsically disordered proteins. *J. Proteome Res.* **2007**, *6*, 1917–1932. [[CrossRef](#)]
80. Xie, H.; Vucetic, S.; Iakoucheva, L.M.; Oldfield, C.J.; Dunker, A.K.; Uversky, V.N.; Obradovic, Z. Functional anthology of intrinsic disorder. 1. Biological processes and functions of proteins with long disordered regions. *J. Proteome Res.* **2007**, *6*, 1882–1898. [[CrossRef](#)]
81. Uversky, V.N.; Oldfield, C.J.; Dunker, A.K. Intrinsically disordered proteins in human diseases: Introducing the D2 concept. *Annu. Rev. Biophys.* **2008**, *37*, 215–246. [[CrossRef](#)]
82. Vacic, V.; Markwick, P.R.; Oldfield, C.J.; Zhao, X.; Haynes, C.; Uversky, V.N.; Iakoucheva, L.M. Disease-associated mutations disrupt functionally important regions of intrinsic protein disorder. *PLoS Comput. Biol.* **2012**, *8*, e1002709. [[CrossRef](#)]
83. Xue, B.; Dunker, A.K.; Uversky, V.N. Orderly order in protein intrinsic disorder distribution: Disorder in 3500 proteomes from viruses and the three domains of life. *J. Biomol. Struct. Dyn.* **2012**, *30*, 137–149. [[CrossRef](#)]
84. Pushker, R.; Mooney, C.; Davey, N.E.; Jacque, J.M.; Shields, D.C. Marked variability in the extent of protein disorder within and between viral families. *PLoS ONE* **2013**, *8*, e60724. [[CrossRef](#)]
85. Morgan, A.R.; Lam, W.J.; Han, D.Y.; Fraser, A.G.; Ferguson, L.R. Genetic variation within TLR10 is associated with Crohn's disease in a New Zealand population. *Hum. Immunol.* **2012**, *73*, 416–420. [[CrossRef](#)]
86. Fore, F.; Indriputri, C.; Mamutse, J.; Nugraha, J. TLR10 and Its Unique Anti-Inflammatory Properties and Potential Use as a Target in Therapeutics. *Immune Netw.* **2020**, *20*, e21. [[CrossRef](#)]
87. Nie, L.; Cai, S.Y.; Shao, J.Z.; Chen, J. Toll-Like Receptors, Associated Biological Roles, and Signaling Networks in Non-Mammals. *Front. Immunol.* **2018**, *9*, 1523. [[CrossRef](#)]

88. Vidya, M.K.; Kumar, V.G.; Sejian, V.; Bagath, M.; Krishnan, G.; Bhatta, R. Toll-like receptors: Significance, ligands, signaling pathways, and functions in mammals. *Int. Rev. Immunol.* **2018**, *37*, 20–36. [[CrossRef](#)]
89. Kawasaki, T.; Kawai, T. Toll-like receptor signaling pathways. *Front. Immunol.* **2014**, *5*, 461. [[CrossRef](#)]
90. Kumar, H.; Kawai, T.; Akira, S. Pathogen recognition by the innate immune system. *Int. Rev. Immunol.* **2011**, *30*, 16–34. [[CrossRef](#)]
91. Jimenez-Dalmaroni, M.J.; Gerswhin, M.E.; Adamopoulos, I.E. The critical role of toll-like receptors—From microbial recognition to autoimmunity: A comprehensive review. *Autoimmun. Rev.* **2016**, *15*, 1–8. [[CrossRef](#)]
92. Takeda, K.; Akira, S. Toll-like receptors. *Curr. Protoc. Immunol.* **2015**, *109*, 14.12.1–14.12.10. [[CrossRef](#)]
93. Kang, J.Y.; Lee, J.O. Structural biology of the Toll-like receptor family. *Annu. Rev. Biochem.* **2011**, *80*, 917–941. [[CrossRef](#)] [[PubMed](#)]
94. Takeda, K.; Akira, S. Toll-like receptors in innate immunity. *Int. Immunol.* **2005**, *17*, 1–14. [[CrossRef](#)] [[PubMed](#)]
95. Blasius, A.L.; Beutler, B. Intracellular toll-like receptors. *Immunity* **2010**, *32*, 305–315. [[CrossRef](#)] [[PubMed](#)]
96. Gay, N.J.; Symmons, M.F.; Gangloff, M.; Bryant, C.E. Assembly and localization of Toll-like receptor signalling complexes. *Nat. Rev. Immunol.* **2014**, *14*, 546–558. [[CrossRef](#)] [[PubMed](#)]
97. Lin, S.C.; Lo, Y.C.; Wu, H. Helical assembly in the MyD88-IRAK4-IRAK2 complex in TLR/IL-1R signalling. *Nature* **2010**, *465*, 885–890. [[CrossRef](#)]
98. Szklarczyk, D.; Franceschini, A.; Kuhn, M.; Simonovic, M.; Roth, A.; Minguéz, P.; Doerks, T.; Stark, M.; Müller, J.; Bork, P.; et al. The STRING database in 2011: Functional interaction networks of proteins, globally integrated and scored. *Nucleic Acids Res.* **2011**, *39*, D561–D568. [[CrossRef](#)]
99. UniProt, C. UniProt: The universal protein knowledgebase in 2021. *Nucleic Acids Res.* **2021**, *49*, D480–D489. [[CrossRef](#)]
100. Duan, T.; Du, Y.; Xing, C.; Wang, H.Y.; Wang, R.F. Toll-Like Receptor Signaling and Its Role in Cell-Mediated Immunity. *Front. Immunol.* **2022**, *13*, 812774. [[CrossRef](#)]
101. Aluri, J.; Cooper, M.A.; Schuettpelez, L.G. Toll-Like Receptor Signaling in the Establishment and Function of the Immune System. *Cells* **2021**, *10*, 1374. [[CrossRef](#)]
102. Capitano, M.L. Toll-like receptor signaling in hematopoietic stem and progenitor cells. *Curr. Opin. Hematol.* **2019**, *26*, 207–213. [[CrossRef](#)]
103. Brennan, J.J.; Gilmore, T.D. Evolutionary Origins of Toll-like Receptor Signaling. *Mol. Biol. Evol.* **2018**, *35*, 1576–1587. [[CrossRef](#)]
104. Satoh, T.; Akira, S. Toll-Like Receptor Signaling and Its Inducible Proteins. *Microbiol. Spectr.* **2016**, *4*, 4–6. [[CrossRef](#)]
105. Leifer, C.A.; Medvedev, A.E. Molecular mechanisms of regulation of Toll-like receptor signaling. *J. Leukoc Biol.* **2016**, *100*, 927–941. [[CrossRef](#)]
106. Piras, V.; Selvarajoo, K. Beyond MyD88 and TRIF Pathways in Toll-Like Receptor Signaling. *Front. Immunol.* **2014**, *5*, 70. [[CrossRef](#)]
107. Lim, K.H.; Staudt, L.M. Toll-like receptor signaling. *Cold Spring Harb. Perspect. Biol.* **2013**, *5*, a011247. [[CrossRef](#)]
108. Qian, C.; Cao, X. Regulation of Toll-like receptor signaling pathways in innate immune responses. *Ann. N. Y. Acad. Sci.* **2013**, *1283*, 67–74. [[CrossRef](#)]
109. Kondo, T.; Kawai, T.; Akira, S. Dissecting negative regulation of Toll-like receptor signaling. *Trends Immunol.* **2012**, *33*, 449–458. [[CrossRef](#)]
110. Yamamoto, M.; Takeda, K. Current views of toll-like receptor signaling pathways. *Gastroenterol. Res. Pract.* **2010**, *2010*, 240365. [[CrossRef](#)]
111. Ostuni, R.; Zanoni, I.; Granucci, F. Deciphering the complexity of Toll-like receptor signaling. *Cell. Mol. Life Sci. CMLS* **2010**, *67*, 4109–4134. [[CrossRef](#)]
112. An, H.; Qian, C.; Cao, X. Regulation of Toll-like receptor signaling in the innate immunity. *Sci. China Life Sci.* **2010**, *53*, 34–43. [[CrossRef](#)]
113. Chaturvedi, A.; Pierce, S.K. How location governs toll-like receptor signaling. *Traffic* **2009**, *10*, 621–628. [[CrossRef](#)]
114. Wang, J.; Hu, Y.; Deng, W.W.; Sun, B. Negative regulation of Toll-like receptor signaling pathway. *Microbes Infect.* **2009**, *11*, 321–327. [[CrossRef](#)]
115. Oda, K.; Kitano, H. A comprehensive map of the toll-like receptor signaling network. *Mol. Syst. Biol.* **2006**, *2*, 2006-0015. [[CrossRef](#)]
116. Akira, S. Toll-like receptor signaling. *J. Biol. Chem.* **2003**, *278*, 38105–38108. [[CrossRef](#)]
117. Ozato, K.; Tsujimura, H.; Tamura, T. Toll-like receptor signaling and regulation of cytokine gene expression in the immune system. *Biotechniques* **2002**, *33*, 66–68; 70; 72. [[CrossRef](#)]
118. Jin, M.S.; Lee, J.O. Structures of the toll-like receptor family and its ligand complexes. *Immunity* **2008**, *29*, 182–191. [[CrossRef](#)]
119. Gay, N.J.; Gangloff, M. Structure and function of Toll receptors and their ligands. *Annu. Rev. Biochem.* **2007**, *76*, 141–165. [[CrossRef](#)]
120. Sandor, F.; Buc, M. Toll-like receptors. I. Structure, function and their ligands. *Folia Biol.* **2005**, *51*, 148–157.
121. O’Neill, L.A.; Bowie, A.G. The family of five: TIR-domain-containing adaptors in Toll-like receptor signalling. *Nat. Rev. Immunol.* **2007**, *7*, 353–364. [[CrossRef](#)]
122. Matsushima, N.; Tanaka, T.; Enkhbayar, P.; Mikami, T.; Taga, M.; Yamada, K.; Kuroki, Y. Comparative sequence analysis of leucine-rich repeats (LRRs) within vertebrate toll-like receptors. *BMC Genom.* **2007**, *8*, 124. [[CrossRef](#)]
123. Kobe, B.; Kajava, A.V. The leucine-rich repeat as a protein recognition motif. *Curr. Opin. Struct. Biol.* **2001**, *11*, 725–732. [[CrossRef](#)]
124. Kajava, A.V. Structural diversity of leucine-rich repeat proteins. *J. Mol. Biol.* **1998**, *277*, 519–527. [[CrossRef](#)] [[PubMed](#)]
125. Wang, J.; Zhang, Z.; Liu, J.; Zhao, J.; Yin, D. Ectodomain Architecture Affects Sequence and Functional Evolution of Vertebrate Toll-like Receptors. *Sci. Rep.* **2016**, *6*, 26705. [[CrossRef](#)] [[PubMed](#)]

126. Underhill, D.M.; Ozinsky, A.; Hajjar, A.M.; Stevens, A.; Wilson, C.B.; Bassetti, M.; Aderem, A. The Toll-like receptor 2 is recruited to macrophage phagosomes and discriminates between pathogens. *Nature* **1999**, *401*, 811–815. [[CrossRef](#)]
127. Palssson-McDermott, E.M.; O'Neill, L.A. Building an immune system from nine domains. *Biochem. Soc. Trans.* **2007**, *35*, 1437–1444. [[CrossRef](#)]
128. Obradovic, Z.; Peng, K.; Vucetic, S.; Radivojac, P.; Dunker, A.K. Exploiting heterogeneous sequence properties improves prediction of protein disorder. *Proteins* **2005**, *61* (Suppl. S7), 176–182. [[CrossRef](#)]
129. Romero, P.; Obradovic, Z.; Li, X.; Garner, E.C.; Brown, C.J.; Dunker, A.K. Sequence complexity of disordered protein. *Proteins* **2001**, *42*, 38–48.
130. Peng, K.; Radivojac, P.; Vucetic, S.; Dunker, A.K.; Obradovic, Z. Length-dependent prediction of protein intrinsic disorder. *BMC Bioinform.* **2006**, *7*, 208. [[CrossRef](#)]
131. Peng, K.; Vucetic, S.; Radivojac, P.; Brown, C.J.; Dunker, A.K.; Obradovic, Z. Optimizing long intrinsic disorder predictors with protein evolutionary information. *J. Bioinform. Comput. Biol.* **2005**, *3*, 35–60. [[CrossRef](#)]
132. Xue, B.; Dunbrack, R.L.; Williams, R.W.; Dunker, A.K.; Uversky, V.N. PONDR-FIT: A meta-predictor of intrinsically disordered amino acids. *Biochim. Biophys. Acta* **2010**, *1804*, 996–1010. [[CrossRef](#)]
133. Dosztanyi, Z.; Csizmok, V.; Tompa, P.; Simon, I. IUPred: Web server for the prediction of intrinsically unstructured regions of proteins based on estimated energy content. *Bioinformatics* **2005**, *21*, 3433–3434. [[CrossRef](#)]
134. Dosztanyi, Z.; Csizmok, V.; Tompa, P.; Simon, I. The pairwise energy content estimated from amino acid composition discriminates between folded and intrinsically unstructured proteins. *J. Mol. Biol.* **2005**, *347*, 827–839. [[CrossRef](#)]
135. Necci, M.; Piovesan, D.; Predictors, C.; DisProt, C.; Tosatto, S.C.E. Critical assessment of protein intrinsic disorder prediction. *Nat. Methods* **2021**, *18*, 472–481. [[CrossRef](#)]
136. Xue, B.; Oldfield, C.J.; Dunker, A.K.; Uversky, V.N. CDF it all: Consensus prediction of intrinsically disordered proteins based on various cumulative distribution functions. *FEBS Lett.* **2009**, *583*, 1469–1474. [[CrossRef](#)]
137. Huang, F.; Oldfield, C.; Meng, J.; Hsu, W.L.; Xue, B.; Uversky, V.N.; Romero, P.; Dunker, A.K. Subclassifying disordered proteins by the CH-CDF plot method. In *Biocomputing*; World Scientific: London, UK, 2012; pp. 128–139.
138. Mohan, A.; Sullivan, W.J., Jr.; Radivojac, P.; Dunker, A.K.; Uversky, V.N. Intrinsic disorder in pathogenic and non-pathogenic microbes: Discovering and analyzing the unfoldomes of early-branching eukaryotes. *Mol. Biosyst.* **2008**, *4*, 328–340. [[CrossRef](#)]
139. Huang, F.; Oldfield, C.J.; Xue, B.; Hsu, W.L.; Meng, J.; Liu, X.; Shen, L.; Romero, P.; Uversky, V.N.; Dunker, A. Improving protein order-disorder classification using charge-hydrophathy plots. *BMC Bioinform.* **2014**, *15* (Suppl. S17), S4. [[CrossRef](#)]
140. Oldfield, C.J.; Cheng, Y.; Cortese, M.S.; Brown, C.J.; Uversky, V.N.; Dunker, A.K. Comparing and combining predictors of mostly disordered proteins. *Biochemistry* **2005**, *44*, 1989–2000. [[CrossRef](#)]
141. He, B.; Wang, K.; Liu, Y.; Xue, B.; Uversky, V.N.; Dunker, A.K. Predicting intrinsic disorder in proteins: An overview. *Cell Res.* **2009**, *19*, 929–949. [[CrossRef](#)]
142. Jumper, J.; Evans, R.; Pritzel, A.; Green, T.; Figurnov, M.; Ronneberger, O.; Tunyasuvunakool, K.; Bates, R.; Zidek, A.; Potapenko, A.; et al. Highly accurate protein structure prediction with AlphaFold. *Nature* **2021**, *596*, 583–589. [[CrossRef](#)]
143. Oates, M.E.; Romero, P.; Ishida, T.; Ghalwash, M.; Mizianty, M.J.; Xue, B.; Dosztanyi, Z.; Uversky, V.N.; Obradovic, Z.; Kurgan, L.; et al. D(2)P(2): Database of disordered protein predictions. *Nucleic Acids Res.* **2013**, *41*, D508–D516. [[CrossRef](#)]
144. Zhou, K.; Kanai, R.; Lee, P.; Wang, H.W.; Modis, Y. Toll-like receptor 5 forms asymmetric dimers in the absence of flagellin. *J. Struct. Biol.* **2012**, *177*, 402–409. [[CrossRef](#)]
145. Ivison, S.M.; Khan, M.A.; Graham, N.R.; Bernales, C.Q.; Kaleem, A.; Tirling, C.O.; Cherkasov, A.; Steiner, T.S. A phosphorylation site in the Toll-like receptor 5 TIR domain is required for inflammatory signalling in response to flagellin. *Biochem. Biophys. Res. Commun.* **2007**, *352*, 936–941. [[CrossRef](#)]
146. Ivison, S.M.; Graham, N.R.; Bernales, C.Q.; Kifayet, A.; Ng, N.; Shobab, L.A.; Steiner, T.S. Protein kinase D interaction with TLR5 is required for inflammatory signaling in response to bacterial flagellin. *J. Immunol.* **2007**, *178*, 5735–5743. [[CrossRef](#)]
147. Iakoucheva, L.M.; Radivojac, P.; Brown, C.J.; O'Connor, T.R.; Sikes, J.G.; Obradovic, Z.; Dunker, A.K. The importance of intrinsic disorder for protein phosphorylation. *Nucleic Acids Res.* **2004**, *32*, 1037–1049. [[CrossRef](#)]
148. Pejaver, V.; Hsu, W.L.; Xin, F.; Dunker, A.K.; Uversky, V.N.; Radivojac, P. The structural and functional signatures of proteins that undergo multiple events of post-translational modification. *Protein Sci.* **2014**, *23*, 1077–1093. [[CrossRef](#)]
149. Darling, A.L.; Uversky, V.N. Intrinsic Disorder and Posttranslational Modifications: The Darker Side of the Biological Dark Matter. *Front. Genet.* **2018**, *9*, 158. [[CrossRef](#)]
150. Jumper, J.; Evans, R.; Pritzel, A.; Green, T.; Figurnov, M.; Ronneberger, O.; Tunyasuvunakool, K.; Bates, R.; Zidek, A.; Potapenko, A.; et al. Applying and improving AlphaFold at CASP14. *Proteins* **2021**, *89*, 1711–1721. [[CrossRef](#)]
151. Ishida, T.; Kinoshita, K. PrDOS: Prediction of disordered protein regions from amino acid sequence. *Nucleic Acids Res.* **2007**, *35*, W460–W464. [[CrossRef](#)]
152. Uversky, V.N. Analyzing IDPs in Interactomes. *Methods Mol. Biol.* **2020**, *2141*, 895–945. [[CrossRef](#)]
153. Walsh, I.; Martin, A.J.; Di Domenico, T.; Tosatto, S.C. ESpritz: Accurate and fast prediction of protein disorder. *Bioinformatics* **2012**, *28*, 503–509. [[CrossRef](#)]
154. Andreeva, A.; Howorth, D.; Brenner, S.E.; Hubbard, T.J.; Chothia, C.; Murzin, A.G. SCOP database in 2004: Refinements integrate structure and sequence family data. *Nucleic Acids Res.* **2004**, *32*, D226–D229. [[CrossRef](#)] [[PubMed](#)]

155. Murzin, A.G.; Brenner, S.E.; Hubbard, T.; Chothia, C. SCOP: A structural classification of proteins database for the investigation of sequences and structures. *J. Mol. Biol.* **1995**, *247*, 536–540. [[CrossRef](#)]
156. de Lima Morais, D.A.; Fang, H.; Rackham, O.J.; Wilson, D.; Pethica, R.; Chothia, C.; Gough, J. SUPERFAMILY 1.75 including a domain-centric gene ontology method. *Nucleic Acids Res.* **2011**, *39*, D427–D434. [[CrossRef](#)] [[PubMed](#)]
157. Meszaros, B.; Simon, I.; Dosztanyi, Z. Prediction of protein binding regions in disordered proteins. *PLoS Comput. Biol.* **2009**, *5*, e1000376. [[CrossRef](#)]
158. Hornbeck, P.V.; Kornhauser, J.M.; Tkachev, S.; Zhang, B.; Skrzypek, E.; Murray, B.; Latham, V.; Sullivan, M. PhosphoSitePlus: A comprehensive resource for investigating the structure and function of experimentally determined post-translational modifications in man and mouse. *Nucleic Acids Res.* **2012**, *40*, D261–D270. [[CrossRef](#)]
159. Patil, A.; Nakamura, H. Disordered domains and high surface charge confer hubs with the ability to interact with multiple proteins in interaction networks. *FEBS Lett.* **2006**, *580*, 2041–2045. [[CrossRef](#)]
160. Ekman, D.; Light, S.; Bjorklund, A.K.; Elofsson, A. What properties characterize the hub proteins of the protein-protein interaction network of *Saccharomyces cerevisiae*? *Genome Biol.* **2006**, *7*, R45. [[CrossRef](#)]
161. Haynes, C.; Oldfield, C.J.; Ji, F.; Klitgord, N.; Cusick, M.E.; Radivojac, P.; Uversky, V.N.; Vidal, M.; Iakoucheva, L.M. Intrinsic disorder is a common feature of hub proteins from four eukaryotic interactomes. *PLoS Comput. Biol.* **2006**, *2*, e100. [[CrossRef](#)]
162. Dosztanyi, Z.; Chen, J.; Dunker, A.K.; Simon, I.; Tompa, P. Disorder and sequence repeats in hub proteins and their implications for network evolution. *J. Proteome Res.* **2006**, *5*, 2985–2995. [[CrossRef](#)]
163. Singh, G.P.; Dash, D. Intrinsic disorder in yeast transcriptional regulatory network. *Proteins* **2007**, *68*, 602–605. [[CrossRef](#)]
164. Singh, G.P.; Ganapathi, M.; Dash, D. Role of intrinsic disorder in transient interactions of hub proteins. *Proteins* **2007**, *66*, 761–765. [[CrossRef](#)]
165. Howell, J.; Angus, P.; Gow, P.; Visvanathan, K. Toll-like receptors in hepatitis C infection: Implications for pathogenesis and treatment. *J. Gastroenterol. Hepatol.* **2013**, *28*, 766–776. [[CrossRef](#)]
166. Luo, L.; Lucas, R.M.; Liu, L.; Stow, J.L. Signalling, sorting and scaffolding adaptors for Toll-like receptors. *J. Cell Sci.* **2019**, *133*, jcs239194. [[CrossRef](#)]
167. Bernard, N.J.; O'Neill, L.A. Mal, more than a bridge to MyD88. *IUBMB Life* **2013**, *65*, 777–786. [[CrossRef](#)]
168. Barnes, B.J.; Moore, P.A.; Pitha, P.M. Virus-specific activation of a novel interferon regulatory factor, IRF-5, results in the induction of distinct interferon alpha genes. *J. Biol. Chem.* **2001**, *276*, 23382–23390. [[CrossRef](#)]
169. Schoenemeyer, A.; Barnes, B.J.; Mancl, M.E.; Latz, E.; Goutagny, N.; Pitha, P.M.; Fitzgerald, K.A.; Golenbock, D.T. The interferon regulatory factor, IRF5, is a central mediator of toll-like receptor 7 signaling. *J. Biol. Chem.* **2005**, *280*, 17005–17012. [[CrossRef](#)]
170. Chang Foreman, H.C.; Van Scoy, S.; Cheng, T.F.; Reich, N.C. Activation of interferon regulatory factor 5 by site specific phosphorylation. *PLoS ONE* **2012**, *7*, e33098. [[CrossRef](#)]
171. Lopez-Pelaez, M.; Lamont, D.J.; Pegg, M.; Shpiro, N.; Gray, N.S.; Cohen, P. Protein kinase IKKbeta-catalyzed phosphorylation of IRF5 at Ser462 induces its dimerization and nuclear translocation in myeloid cells. *Proc. Natl. Acad. Sci. USA* **2014**, *111*, 17432–17437. [[CrossRef](#)]
172. Heinz, L.X.; Lee, J.; Kapoor, U.; Kartnig, F.; Sedlyarov, V.; Papakostas, K.; Cesar-Razquin, A.; Essletzbichler, P.; Goldmann, U.; Stefanovic, A.; et al. TASL is the SLC15A4-associated adaptor for IRF5 activation by TLR7-9. *Nature* **2020**, *581*, 316–322. [[CrossRef](#)]
173. Vallance, T.M.; Zeuner, M.T.; Williams, H.F.; Widera, D.; Vaiyapuri, S. Toll-Like Receptor 4 Signalling and Its Impact on Platelet Function, Thrombosis, and Haemostasis. *Mediat. Inflamm.* **2017**, *2017*, 9605894. [[CrossRef](#)]
174. Billod, J.M.; Lacetera, A.; Guzman-Caldentey, J.; Martin-Santamaria, S. Computational Approaches to Toll-Like Receptor 4 Modulation. *Molecules* **2016**, *21*, 994. [[CrossRef](#)] [[PubMed](#)]
175. Hacker, H.; Tseng, P.H.; Karin, M. Expanding TRAF function: TRAF3 as a tri-faced immune regulator. *Nat. Rev. Immunol.* **2011**, *11*, 457–468. [[CrossRef](#)] [[PubMed](#)]
176. Jenkins, K.A.; Mansell, A. TIR-containing adaptors in Toll-like receptor signalling. *Cytokine* **2010**, *49*, 237–244. [[CrossRef](#)] [[PubMed](#)]
177. Horner, S.M.; Gale, M., Jr. Regulation of hepatic innate immunity by hepatitis C virus. *Nat. Med.* **2013**, *19*, 879–888. [[CrossRef](#)]
178. Chuang, T.; Ulevitch, R.J. Identification of hTLR10: A novel human Toll-like receptor preferentially expressed in immune cells. *Biochim. Biophys. Acta* **2001**, *1518*, 157–161. [[CrossRef](#)]
179. Henrick, B.M.; Yao, X.D.; Zahoor, M.A.; Abimiku, A.; Osawe, S.; Rosenthal, K.L. TLR10 Senses HIV-1 Proteins and Significantly Enhances HIV-1 Infection. *Front. Immunol.* **2019**, *10*, 482. [[CrossRef](#)]
180. Oosting, M.; Cheng, S.C.; Bolscher, J.M.; Vestering-Stenger, R.; Plantinga, T.S.; Verschuere, I.C.; Arts, P.; Garritsen, A.; van Eenennaam, H.; Sturm, P.; et al. Human TLR10 is an anti-inflammatory pattern-recognition receptor. *Proc. Natl. Acad. Sci. USA* **2014**, *111*, E4478–E4484. [[CrossRef](#)]
181. Sindhu, S.; Akhter, N.; Kochumon, S.; Thomas, R.; Wilson, A.; Shenouda, S.; Tuomilehto, J.; Ahmad, R. Increased Expression of the Innate Immune Receptor TLR10 in Obesity and Type-2 Diabetes: Association with ROS-Mediated Oxidative Stress. *Cell Physiol. Biochem.* **2018**, *45*, 572–590. [[CrossRef](#)]
182. Torices, S.; Julia, A.; Munoz, P.; Varela, I.; Balsa, A.; Marsal, S.; Fernandez-Nebro, A.; Blanco, F.; Lopez-Hoyos, M.; Martinez-Taboada, V.; et al. A functional variant of TLR10 modifies the activity of NFkB and may help predict a worse prognosis in patients with rheumatoid arthritis. *Arthritis Res.* **2016**, *18*, 221. [[CrossRef](#)]

183. Kim, D.; Kim, Y.J.; Koh, H.S.; Jang, T.Y.; Park, H.E.; Kim, J.Y. Reactive oxygen species enhance TLR10 expression in the human monocytic cell line THP-1. *Int. J. Mol. Sci.* **2010**, *11*, 3769–3782. [[CrossRef](#)]
184. Hasan, U.; Chaffois, C.; Gaillard, C.; Saulnier, V.; Merck, E.; Tancredi, S.; Guiet, C.; Briere, F.; Vlach, J.; Lebecque, S.; et al. Human TLR10 is a functional receptor, expressed by B cells and plasmacytoid dendritic cells, which activates gene transcription through MyD88. *J. Immunol.* **2005**, *174*, 2942–2950. [[CrossRef](#)]
185. Tarlinton, R.E.; Alder, L.; Moreton, J.; Maboni, G.; Emes, R.D.; Totemeyer, S. RNA expression of TLR10 in normal equine tissues. *BMC Res. Notes* **2016**, *9*, 353. [[CrossRef](#)]
186. Chang, S.; Dolganiuc, A.; Szabo, G. Toll-like receptors 1 and 6 are involved in TLR2-mediated macrophage activation by hepatitis C virus core and NS3 proteins. *J. Leukoc Biol.* **2007**, *82*, 479–487. [[CrossRef](#)]
187. Farhat, K.; Riekenberg, S.; Heine, H.; Debarry, J.; Lang, R.; Mages, J.; Buwitt-Beckmann, U.; Roschmann, K.; Jung, G.; Wiesmuller, K.H.; et al. Heterodimerization of TLR2 with TLR1 or TLR6 expands the ligand spectrum but does not lead to differential signaling. *J. Leukoc Biol.* **2008**, *83*, 692–701. [[CrossRef](#)]
188. Coenen, M.; Nischalke, H.D.; Kramer, B.; Langhans, B.; Glassner, A.; Schulte, D.; Korner, C.; Sauerbruch, T.; Nattermann, J.; Spengler, U. Hepatitis C virus core protein induces fibrogenic actions of hepatic stellate cells via toll-like receptor 2. *Lab. Invest.* **2011**, *91*, 1375–1382. [[CrossRef](#)]
189. Seki, E.; Schwabe, R.F. Hepatic inflammation and fibrosis: Functional links and key pathways. *Hepatology* **2015**, *61*, 1066–1079. [[CrossRef](#)]
190. Rajagopalan, K.; Mooney, S.M.; Parekh, N.; Getzenberg, R.H.; Kulkarni, P. A majority of the cancer/testis antigens are intrinsically disordered proteins. *J. Cell Biochem.* **2011**, *112*, 3256–3267. [[CrossRef](#)]
191. Sene, D.; Levasseur, F.; Abel, M.; Lambert, M.; Camous, X.; Hernandez, C.; Pene, V.; Rosenberg, A.R.; Jouvin-Marche, E.; Marche, P.N.; et al. Hepatitis C virus (HCV) evades NKG2D-dependent NK cell responses through NS5A-mediated imbalance of inflammatory cytokines. *PLoS Pathog.* **2010**, *6*, e1001184. [[CrossRef](#)]
192. Machida, K.; Cheng, K.T.; Sung, V.M.; Levine, A.M.; Fong, S.; Lai, M.M. Hepatitis C virus induces toll-like receptor 4 expression, leading to enhanced production of beta interferon and interleukin-6. *J. Virol.* **2006**, *80*, 866–874. [[CrossRef](#)]
193. Tamura, R.; Kanda, T.; Imazeki, F.; Wu, S.; Nakamoto, S.; Tanaka, T.; Arai, M.; Fujiwara, K.; Saito, K.; Roger, T.; et al. Hepatitis C Virus nonstructural 5A protein inhibits lipopolysaccharide-mediated apoptosis of hepatocytes by decreasing expression of Toll-like receptor 4. *J. Infect. Dis.* **2011**, *204*, 793–801. [[CrossRef](#)]
194. Li, K.; Foy, E.; Ferreon, J.C.; Nakamura, M.; Ferreon, A.C.; Ikeda, M.; Ray, S.C.; Gale, M., Jr.; Lemon, S.M. Immune evasion by hepatitis C virus NS3/4A protease-mediated cleavage of the Toll-like receptor 3 adaptor protein TRIF. *Proc. Natl. Acad. Sci. USA* **2005**, *102*, 2992–2997. [[CrossRef](#)]
195. Broering, R.; Lu, M.; Schlaak, J.F. Role of Toll-like receptors in liver health and disease. *Clin. Sci.* **2011**, *121*, 415–426. [[CrossRef](#)] [[PubMed](#)]
196. Moriyama, M.; Kato, N.; Otsuka, M.; Shao, R.X.; Taniguchi, H.; Kawabe, T.; Omata, M. Interferon-beta is activated by hepatitis C virus NS5B and inhibited by NS4A, NS4B, and NS5A. *Hepatol. Int.* **2007**, *1*, 302–310. [[CrossRef](#)] [[PubMed](#)]
197. Mohamed, A.A.; Omran, D.; El-Feky, S.; Darwish, H.; Kassas, A.; Farouk, A.; Ezzat, O.; Abdo, S.M.; Zahran, F.E.; El-Demery, A.; et al. Toll-like receptor 7 mRNA is reduced in hepatitis C-based liver cirrhosis and hepatocellular carcinoma, out-performs alpha-fetoprotein levels, and with age and serum aspartate aminotransferase is a new diagnostic index. *Br. J. Biomed. Sci.* **2021**, *78*, 18–22. [[CrossRef](#)] [[PubMed](#)]
198. Abe, T.; Kaname, Y.; Hamamoto, I.; Tsuda, Y.; Wen, X.; Taguwa, S.; Moriishi, K.; Takeuchi, O.; Kawai, T.; Kanto, T.; et al. Hepatitis C virus nonstructural protein 5A modulates the toll-like receptor-MyD88-dependent signaling pathway in macrophage cell lines. *J. Virol.* **2007**, *81*, 8953–8966. [[CrossRef](#)] [[PubMed](#)]
199. Chowdhury, J.B.; Kim, H.; Ray, R.; Ray, R.B. Hepatitis C virus NS5A protein modulates IRF-7-mediated interferon-alpha signaling. *J. Interferon Cytokine Res.* **2014**, *34*, 16–21. [[CrossRef](#)]
200. Sun, L.; Dai, J.J.; Hu, W.F.; Wang, J. Expression of toll-like receptors in hepatic cirrhosis and hepatocellular carcinoma. *Genet. Mol. Res.* **2016**, *15*, 7419. [[CrossRef](#)]
201. Watanabe, A.; Hashmi, A.; Gomes, D.A.; Town, T.; Badou, A.; Flavell, R.A.; Mehal, W.Z. Apoptotic hepatocyte DNA inhibits hepatic stellate cell chemotaxis via toll-like receptor 9. *Hepatology* **2007**, *46*, 1509–1518. [[CrossRef](#)]
202. Zhou, J.; Huang, Y.; Tian, D.; Xu, D.; Chen, M.; Wu, H. Expression of toll-like receptor 9 in peripheral blood mononuclear cells from patients with different hepatitis B and C viral loads. *J. Huazhong Univ. Sci. Technol. Med. Sci.* **2009**, *29*, 313–317. [[CrossRef](#)]
203. Smith, L.M.; Kelleher, N.L.; Consortium for Top Down, P. Proteoform: A single term describing protein complexity. *Nat. Methods* **2013**, *10*, 186–187. [[CrossRef](#)]
204. Uversky, V.N. Protein intrinsic disorder and structure-function continuum. *Prog. Mol. Biol. Transl. Sci.* **2019**, *166*, 1–17. [[CrossRef](#)]
205. Fonin, A.V.; Darling, A.L.; Kuznetsova, I.M.; Turoverov, K.K.; Uversky, V.N. Multi-functionality of proteins involved in GPCR and G protein signaling: Making sense of structure-function continuum with intrinsic disorder-based proteoforms. *Cell. Mol. Life Sci. CMLS* **2019**, *76*, 4461–4492. [[CrossRef](#)]
206. Weisz, J.; Uversky, V.N. Zooming into the Dark Side of Human Annexin-S100 Complexes: Dynamic Alliance of Flexible Partners. *Int. J. Mol. Sci.* **2020**, *21*, 5879. [[CrossRef](#)]
207. Uversky, V.N.; Dave, V.; Iakoucheva, L.M.; Malaney, P.; Metallo, S.J.; Pathak, R.R.; Joerger, A.C. Pathological unfoldomics of uncontrolled chaos: Intrinsically disordered proteins and human diseases. *Chem. Rev.* **2014**, *114*, 6844–6879. [[CrossRef](#)]

208. Midic, U.; Oldfield, C.J.; Dunker, A.K.; Obradovic, Z.; Uversky, V.N. Unfoldomics of human genetic diseases: Illustrative examples of ordered and intrinsically disordered members of the human diseasome. *Protein Pept. Lett.* **2009**, *16*, 1533–1547. [[CrossRef](#)]
209. Uversky, V.N. Intrinsic disorder in proteins associated with neurodegenerative diseases. *Front. Biosci.* **2009**, *14*, 5188–5238. [[CrossRef](#)]
210. Uversky, V.N.; Oldfield, C.J.; Midic, U.; Xie, H.; Xue, B.; Vucetic, S.; Iakoucheva, L.M.; Obradovic, Z.; Dunker, A.K. Unfoldomics of human diseases: Linking protein intrinsic disorder with diseases. *BMC Genom.* **2009**, *10* (Suppl. S1), S7. [[CrossRef](#)]
211. Uversky, V.N. Targeting intrinsically disordered proteins in neurodegenerative and protein dysfunction diseases: Another illustration of the D(2) concept. *Expert Rev. Proteom.* **2010**, *7*, 543–564. [[CrossRef](#)]
212. Uversky, V.N. Wrecked regulation of intrinsically disordered proteins in diseases: Pathogenicity of deregulated regulators. *Front. Mol. Biosci.* **2014**, *1*, 6. [[CrossRef](#)]
213. Uversky, V.N.; Roman, A.; Oldfield, C.J.; Dunker, A.K. Protein intrinsic disorder and human papillomaviruses: Increased amount of disorder in E6 and E7 oncoproteins from high risk HPVs. *J. Proteome Res.* **2006**, *5*, 1829–1842. [[CrossRef](#)]
214. Goh, G.K.; Dunker, A.K.; Uversky, V.N. Protein intrinsic disorder and influenza virulence: The 1918 H1N1 and H5N1 viruses. *Viol. J.* **2009**, *6*, 69. [[CrossRef](#)]
215. Xue, B.; Mizianty, M.J.; Kurgan, L.; Uversky, V.N. Protein intrinsic disorder as a flexible armor and a weapon of HIV-1. *Cell. Mol. Life Sci. CMLS* **2012**, *69*, 1211–1259. [[CrossRef](#)]
216. Meng, F.; Badierah, R.A.; Almehdar, H.A.; Redwan, E.M.; Kurgan, L.; Uversky, V.N. Unstructural biology of the Dengue virus proteins. *FEBS J.* **2015**, *282*, 3368–3394. [[CrossRef](#)]
217. Whelan, J.N.; Reddy, K.D.; Uversky, V.N.; Teng, M.N. Functional correlations of respiratory syncytial virus proteins to intrinsic disorder. *Mol. Biosyst.* **2016**, *12*, 1507–1526. [[CrossRef](#)]
218. Mishra, P.M.; Uversky, V.N.; Giri, R. Molecular Recognition Features in Zika Virus Proteome. *J. Mol. Biol.* **2018**, *430*, 2372–2388. [[CrossRef](#)]
219. Giri, R.; Kumar, D.; Sharma, N.; Uversky, V.N. Intrinsically Disordered Side of the Zika Virus Proteome. *Front. Cell Infect. Microbiol.* **2016**, *6*, 144. [[CrossRef](#)]
220. Redwan, E.M.; AlJaddawi, A.A.; Uversky, V.N. Structural disorder in the proteome and interactome of Alkhurma virus (ALKV). *Cell. Mol. Life Sci. CMLS* **2019**, *76*, 577–608. [[CrossRef](#)] [[PubMed](#)]
221. Singh, A.; Kumar, A.; Uversky, V.N.; Giri, R. Understanding the interactability of chikungunya virus proteins via molecular recognition feature analysis. *RSC Adv.* **2018**, *8*, 27293–27303. [[CrossRef](#)] [[PubMed](#)]
222. Kumar, D.; Singh, A.; Kumar, P.; Uversky, V.N.; Rao, C.D.; Giri, R. Understanding the penetrance of intrinsic protein disorder in rotavirus proteome. *Int. J. Biol. Macromol.* **2020**, *144*, 892–908. [[CrossRef](#)] [[PubMed](#)]
223. Bhardwaj, T.; Saumya, K.U.; Kumar, P.; Sharma, N.; Gadhav, K.; Uversky, V.N.; Giri, R. Japanese encephalitis virus—Exploring the dark proteome and disorder-function paradigm. *FEBS J.* **2020**, *287*, 3751–3776. [[CrossRef](#)]
224. Giri, R.; Bhardwaj, T.; Shegane, M.; Gehi, B.R.; Kumar, P.; Gadhav, K.; Oldfield, C.J.; Uversky, V.N. Understanding COVID-19 via comparative analysis of dark proteomes of SARS-CoV-2, human SARS and bat SARS-like coronaviruses. *Cell. Mol. Life Sci. CMLS* **2021**, *78*, 1655–1688. [[CrossRef](#)] [[PubMed](#)]
225. Anjum, F.; Mohammad, T.; Asrani, P.; Shafie, A.; Singh, S.; Yadav, D.K.; Uversky, V.N.; Hassan, M.I. Identification of intrinsically disordered regions in non-structural proteins of SARS-CoV-2: New insights into drug and vaccine resistance. *Mol. Cell Biochem.* **2022**, *477*, 1607–1619. [[CrossRef](#)] [[PubMed](#)]
226. Alshehri, M.A.; Manee, M.M.; Alqahtani, F.H.; Al-Shomrani, B.M.; Uversky, V.N. On the Prevalence and Potential Functionality of an Intrinsic Disorder in the MERS-CoV Proteome. *Viruses* **2021**, *13*, 339. [[CrossRef](#)] [[PubMed](#)]
227. Uversky, V.N.; Redwan, E.M.; Aljadawi, A.A. Protein Intrinsic Disorder and Evolvability of MERS-CoV. *Biomolecules* **2021**, *11*, 608. [[CrossRef](#)]
228. Sharma, N.R.; Gadhav, K.; Kumar, P.; Saif, M.; Khan, M.M.; Sarkar, D.P.; Uversky, V.N.; Giri, R. Analysis of the dark proteome of Chandipura virus reveals maximum propensity for intrinsic disorder in phosphoprotein. *Sci. Rep.* **2021**, *11*, 13253. [[CrossRef](#)]
229. Xue, B.; Ganti, K.; Rabionet, A.; Banks, L.; Uversky, V.N. Disordered interactome of human papillomavirus. *Curr. Pharm. Des.* **2014**, *20*, 1274–1292. [[CrossRef](#)]
230. Xue, B.; Uversky, V.N. Intrinsic disorder in proteins involved in the innate antiviral immunity: Another flexible side of a molecular arms race. *J. Mol. Biol.* **2014**, *426*, 1322–1350. [[CrossRef](#)]
231. Kumar, N.; Kaushik, R.; Tennakoon, C.; Uversky, V.N.; Longhi, S.; Zhang, K.Y.J.; Bhatia, S. Comprehensive Intrinsic Disorder Analysis of 6108 Viral Proteomes: From the Extent of Intrinsic Disorder Penetrance to Functional Annotation of Disordered Viral Proteins. *J. Proteome Res.* **2021**, *20*, 2704–2713. [[CrossRef](#)]